



# Modeling, multi-objective optimization and comparison of fire and water tube heat recovery steam generators for gas engine cogeneration plants

Sepehr Sanaye<sup>1</sup> · Ali Ghaffari<sup>1</sup>

Received: 19 September 2020 / Accepted: 21 December 2020 / Published online: 5 February 2021  
© Akadémiai Kiadó, Budapest, Hungary 2021

## Abstract

An innovative modeling and optimizing of fire and water tube heat recovery steam generators (HRSG) for gas engine cogeneration plant are performed here. In modeling section, the equations of  $\varepsilon$ -NTU, LMTD and heat transfer coefficients for one-phase flow and two-phase flow are organized to form a nonlinear system of equations. Furthermore, in the next step, two pairs of objective functions (annual expenses—exergy destruction rate and annual expenses—thermal effectiveness) are selected for multi-objective optimization of HRSG by the use of genetic algorithm for one, two and three MW gas engine cogeneration plants. Results for a 2 MW gas engine (as an example) show that the fire tube HRSG total expenses are 50% lower than that for water tube HRSG. In this situation, for water and fire tube boilers, the effectiveness and cost are 0.9, 40,000 (\$/year) and 0.9, 20,000 (\$/year), respectively. Furthermore, the exergy destruction rates are close and equal to 1373.45 kW and 1366.2 kW for water tube and fire tube boilers, respectively. Moreover, for each gas engine, six equations with thirty constant coefficients are obtained to explain the behavior of HRSG outlet exhaust gas temperature, pinch temperature difference, steam generation mass flow rate, working pressure, thermal effectiveness and exergy destruction rate at partial load.

**Keywords** Heat recovery steam generator · Gas engine · Partial load · Evolutionary algorithm · Exergo-economic optimization

## List of symbols

$A$	Heat transfer surface area ( $\text{m}^2$ )	$H$	Annual working hours of HRSG (h)
$C_p$	Specific heat capacity ( $\text{kJ kg}^{-1} \text{K}^{-1}$ )	$h$	Specific enthalpy ( $\text{kJ kg}^{-1}$ )
CI	Cost index	$h_{fg}$	Latent heat of vaporization ( $\text{kJ kg}^{-1}$ )
CRF	Capital recovery factor	$h_i$	Heat transfer coefficient inside tubes ( $\text{W m}^{-2} \text{K}^{-1}$ )
$C_{\text{Total}}$	Total annual cost of HRSG ( $\text{\$/year}^{-1}$ )	$h_k(x)$	Unequal constraints
$d$	Diameter of the tubes (cm)	$h_o$	Heat transfer coefficient outside tubes ( $\text{W m}^{-2} \text{K}^{-1}$ )
$\dot{E}$	Exergy destruction/loss rate (kW)	$i$	Interest rate
$F$	Logarithmic mean temperature difference correction factor	$k$	Thermal conductivity ( $\text{W m}^{-1} \text{K}^{-1}$ )
$f_i(x)$	Objective functions	$K_{\text{Eco}}$	Economizer unit price of surface area ( $\text{\$/m}^2$ )
$f_g$	Friction coefficient	$K_{\text{Eva}}$	Evaporator unit price of surface area ( $\text{\$/m}^2$ )
$ff_i$	Internal fouling factor ( $\text{m}^2 \text{K W}^{-1}$ )	$K_{\text{Sh}}$	Superheater unit price of surface area ( $\text{\$/m}^2$ )
$ff_o$	External fouling factor ( $\text{m}^2 \text{K W}^{-1}$ )	$L$	Length of the tubes (m)
$G$	Mass velocity ( $\text{kg m}^{-2} \text{s}^{-1}$ )	$\dot{m}_g$	Gas mass flow rate ( $\text{kg s}^{-1}$ )
$g_j(x)$	Equal constraints	$\dot{m}_s$	Steam flow rate ( $\text{kg s}^{-1}$ )
		$N_{\text{obj}}(x)$	Number of objectives
		$N_{\text{par}}$	Number of design parameters
		$N_w$	Number of tubes per width
		NDOB	Non-dimensional objective function
		NU	Nusselt number
		$n$	Equipment lifetime (year)

✉ Sepehr Sanaye  
sepehr@iust.ac.ir

<sup>1</sup> Energy Systems Improvement Laboratory (ESIL), School of Mechanical Engineering, Iran University of Science and Technology (IUST), Narmak, Tehran, Iran

$P$	Pressure (Pa)
PL	Partial load (%)
Pr	Prandtl number
$\dot{Q}$	Heat transfer rate (kW)
$q$	Thermal flux ( $\text{W m}^{-2}$ )
Re	Reynolds number
$S_T$	Transversal pitch (m)
$S_L$	Longitudinal pitch (m)
$s$	Specific entropy ( $\text{J K}^{-1} \text{kg}^{-1}$ )
$T$	Temperature ( $^{\circ}\text{C}$ )
THP	Thermodynamic parameter
TR	Wall thermal resistance ( $\text{m}^2 \text{K W}^{-1}$ )
$U$	Overall heat transfer coefficient ( $\text{W m}^{-2} \text{K}^{-1}$ )
$V$	Velocity ( $\text{m s}^{-1}$ )
$W$	Mass coefficient of water and steam
$X$	Design parameter vectors

### Greek symbols

$\alpha$	Cost factor used in cost objective function
$\Delta p_g$	Gas side pressure drop (kPa)
$\Delta T_m$	Logarithmic mean temperature difference
$\Delta W$	Power loss (W)
$\rho$	Density ( $\text{kg m}^{-3}$ )
$\varepsilon$	Thermal effectiveness
$\eta$	Efficiency
$\mu$	Dynamics viscosity (Pa s)

### Subscripts

am	Ambient
atm	Atmosphere
b	Bulk
CC	Capital cost
CHP	Combined heat and power
d	Design mode
Eco	Economizer
Eva	Evaporator
GE	Gas engine
$g_1$	Gas entering the superheater
$g_2$	Gas entering the evaporator
$g_3$	Gas entering the economizer
$g_4$	Gas leaving the economizer
HRSG	Heat recovery steam generator
LMTD	Logarithmic mean temperature difference
Min	Minimum
Max	Maximum
NSGA	Non-dominated sorting genetic algorithm
NTU	Number of transfer unit
p	Partial mode
sat	Saturation state
Sh	Superheater
st	Steam
w	Wall

## Introduction

Heat recovery from gas engine exhaust gases in CHP systems leads to 80% increase in system overall efficiency [1]. There are many available research studies in which heat recovery from reciprocating engine exhaust gases is investigated by the use of water or fire tube heat recovery boiler. These references are categorized in below.

### Heat recovery by water tube boiler (WTB)

Capata and Toro [2] studied sensible exhaust gas heat recovery from a 1400 CC diesel engine and 30–50 kW micro gas turbine for power generation using steam Rankine cycle. Optimization of water tube HRSG was done with design parameters including tube numbers, tube internal diameter, shell side internal diameter, baffle numbers and space between two baffles in order to reduce the size of heat exchanger. Nadir and Ghenaiet [3] performed optimization of a water tube HRSG by utilizing particle swarm optimization algorithm. The results showed that adding the pressure levels leads to the increase of pressure of high-pressure turbine, power generation and produced specific work and decrease of the exergy losses.

Thermo-economic optimization of a water tube HRSG is conducted by Franco and Russo [4]. Their results showed that the above approach in system analysis increased the system thermal efficiency for 60% due to the heat transfer surface increment and the pinch point decrement.

Rezaei et al. [5] optimized a water tube HRSG including two superheaters, one evaporator and one economizer using single-objective (capital investment cost) genetic algorithm. The optimization variables include the fin tube arrangement, approach point, pinch point, water and steam velocity. Their results showed that the presented optimization method leads to the decrement of the total heat transfer surface area and consequently the capital cost by 22.3% and 24.3%, respectively.

Carapellucci and Giordano [6] optimized a water tube HRSG using two methods. First method minimizes the electricity generation unit cost and second method minimizes an exergo-economic objective function (investment and operational, fuel consumption and exergy destruction costs). Design parameters were pinch point temperature, drum pressure, superheat degree, pressure level numbers and flow arrangement. The best configuration and arrangement of HRSG's heat exchangers are achieved. Nadir et al. [7] analyzed the effect of electricity selling tariff on optimum design parameters of water tube HRSG and ideal configuration selection for different range of exhaust gas

temperatures. Optimization was done once with steam cycle specific work (which was maximized), once with net present value (which was maximized) and once with both functions using PSO algorithm. The best configuration of HRSG (one, two and three pressure levels) is obtained regarding the selling electricity tariff from thermodynamic and economic points of view. Kaviri et al. [8] optimized a dual pressure HRSG considering the exergy destruction per inlet gas as objective function and the drum pressure, pinch point temperature and steam mass flow rates as design parameters. The results showed that the increase of inlet gas temperature up to 650 °C leads to the cycle energy and exergy efficiency increment. Exergo-economic multi-objective optimization of a water tube HRSG is performed by Nikbakht Naserabad et al. [9] using genetic algorithm method in order to repower the steam Rankine cycle. They showed that the exergy efficiency of the plant increased to more than 46% by the presented optimization method. Ahmed et al. [10] proposed a design methodology for a dual pressure HRSG used in a combined cycle power plant with a 60 MW gas turbine. The results showed that the maximum heat transfer occurs in the evaporator section for high-pressure levels, and in the economizer section for low-pressure levels.

Mokhtari et al. [11] carried out 4E analysis and genetic algorithm optimization of a water tube HRSG with two pressure levels. They showed that the optimized design of HRSG decreases the gas turbine power loss and increases the exergy and thermal efficiencies from 42% and 47.6% to 47.28% and 48.94%, respectively.

### Heat recovery by fire tube boiler (FTB)

Fire tube boilers are used broadly in CHP systems; however, there are a lower number of published research studies regarding this type of boilers in comparison with that for water tube boilers. Behbahani-nia and Bagheri [12] optimized a fire tube HRSG in 600 kW micro-turbine cogeneration power generation plant considering exergy losses and annual costs of HRSG as objective functions utilizing genetic algorithm. Thermodynamic, thermo-economic and multi-objective optimization were performed for system analysis. The results showed that thermo-economic and multi-objective optimization provides the total cost decrement due to decreasing in the cost of energy loss as well as decrease in the pinch point. Najafi [13] optimized a fire tube HRSG with considering tube numbers in a row, tube length, tube transverse pitch and pinch point temperature as design variables, while the second law efficiency and investment cost were as objective functions. They showed that the geometric configurations which give higher second law efficiency lead to more expensive design.

Cogeneration systems have been also studied by various types of analyses such as energy and exergy [14–18], exergy-economic [4, 5, 12, 13, 19], energy-economic [20, 21] and entropy-economic aspects [5, 15]. Prime movers in these systems were gas/micro gas turbines [2, 4, 8, 12, 19, 22] as well as diesel engines [23–25]. Authors could not find in literature the subject of simultaneous 3E modeling and optimizing of HRSG in a gas engine CHP system. Furthermore, to the best of our knowledge, no work could be found on simultaneous optimization and comparison of water tube and fire tube HRSGs in a gas engine cogeneration plant. Moreover, the discussions of water tube HRSG in literature are mainly focused on its application in combined cycle power plants (with gas turbine having high exhaust gas temperature for producing steam with low-, intermediate- and high-pressure levels). This is while that the fire tube boilers may be more suitable for small CHP systems (range of 50 kW to 25 MW) in which the steam pressure and exhaust gas temperature of prime mover are lower than that for combined cycle power plants. The comparison of modeling and optimizing results for two types of water tube and fire tube boilers with one similar approach and similar input values (the same inlet hot gas temperatures and mass flow rates) also cannot be found in literature. Finally, the above analysis is carried out for CHP systems with 1, 2 and 3 MW gas engines to illustrate its ability in designing a HRSG with higher energy and exergy efficiencies and lower total costs.

The main contributions of the present work are explained in the following:

- (a) In energy modeling, a new algorithm (which is described in HRSG thermal modeling section) is presented for solving the conservation equations in energy or thermal modeling section. This algorithm combines  $\varepsilon$ -NTU (which helps to speed up reaching the convergence in solving equations in superheater and economizer) and LMTD (which helps to speed up solving equations of evaporator without iteration) methods to form a nonlinear system of equations. The system of equations also uses the precise heat transfer coefficients for one-phase flow (economizer and superheater) and two-phase flow (evaporator) for both water tube and fire tube HRSGs. Thus with input parameters such as the inlet hot gas mass flow rate and temperature besides feed water temperature, the output parameters including equipment outlet gas, water and steam temperatures, produced steam mass flow rate, equipment heat transfer rate and heat transfer surface area are obtained. With the presented algorithm, the performance parameters as well as sizing and rating of water or fire tube HRSG are accomplished with satisfied speed and accuracy. Moreover, the exergy and economic modeling of HRSG system are also performed; thus, modeling of

both types of water tube and fire tube HRSGs for gas engine cogeneration plants is presented in three aspects of energy, exergy and economic.

- (b) In the optimization process, two pairs of objective functions, thermal effectiveness—total annual cost and exergy destruction rate—total annual cost are applied, and a set of design variables for geometry and working conditions (including temperatures and pressures) are selected for both fire and water tube boilers. It is shown that using total annual cost as the first objective function and thermal effectiveness or exergy destruction rate as the second objective function result in relatively close values for optimum design variables and objective functions. Reaching similar optimum solution by choosing two pairs of objective functions in this paper revealed that design variables, constraints and genetic algorithm tuning parameters, are selected appropriately for the integrated system. This result verifies the optimization procedure.
- (c) One important application of the presented modeling and optimizing process is that the HRSG can be optimally designed for specific customer demands. In this regard, in addition to the optimization of HRSG for heat recovery from a specific gas engine (consider as scenario A), system optimization with a specified outlet steam pressure (scenario B) and optimization with specified steam mass flow rate (scenario C) for 2 MW gas engine are performed and the results are compared. It will be shown that in scenario A, the thermal effectiveness is higher and total annual cost as well as exergy destruction rate are lower than that for two other case studies.
- (d) The performance of the optimized fire tube HRSG in four partial loads (90%, 80%, 70% and 60%) is also evaluated. Six relations are proposed for six perfor-

mance parameters in the form of fourth-degree polynomials. These parameters are HRSG outlet exhaust gas temperature, pinch temperature difference, steam generation mass flow rate, working pressure, thermal effectiveness and exergy destruction rate versus the engine load variations. The constant coefficients for estimation of the above performance parameters are reported and can be used for specifying the operating conditions of HRSG in gas engine cogeneration plants.

All above points are innovative concepts which were not observed in open literature. Furthermore, it should be noted that there is no professional software for optimization of gas engine heat recovery system.

## System modeling and analysis

Figures 1 and 2 show water tube and fire tube HRSG with economizer, evaporator and superheater sections for heat recovery application, respectively. The evaporator section has different structure in these two types of HRSG. In HRSG with fire tube type, engine exhaust gasses pass through inside tube of evaporator, while in HRSG with water tube type, exhaust gasses pass over evaporator tube bank.

## Energy modeling and analysis

### HRSG thermal modeling

In HRSG thermal modeling, parameters such as the exit gas temperature from economizer, evaporator and superheater as well as the superheat steam temperature, steam mass flow rate and heat transfer surface area should be estimated.

**Fig. 1** The schematic diagram for a water tube heat recovery steam generator

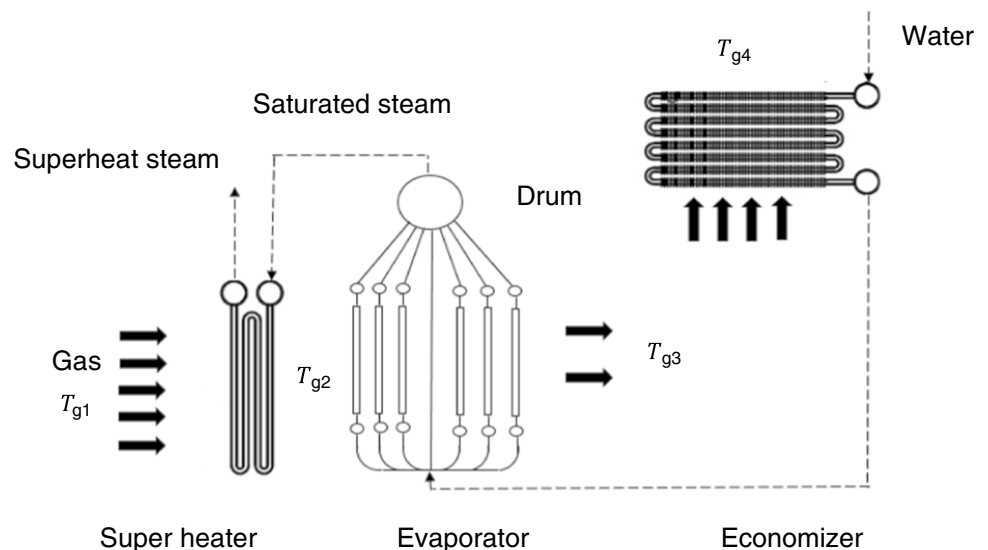
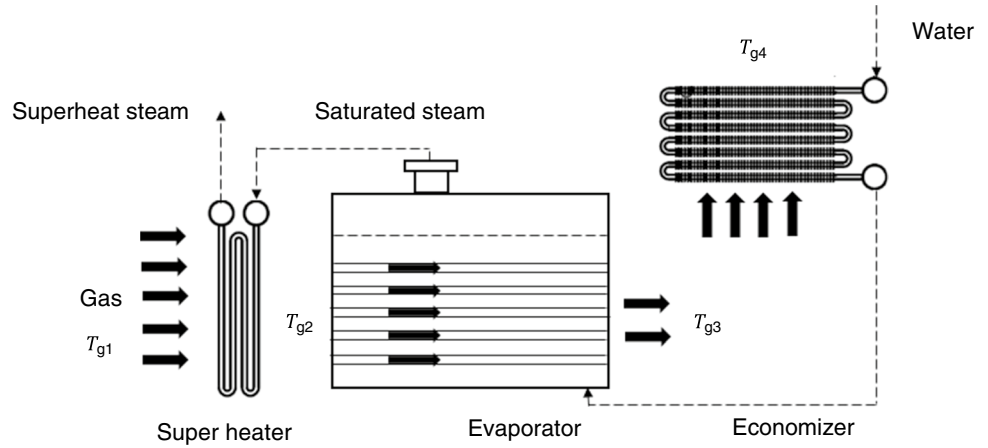


**Fig. 2** The schematic diagram for a fire tube heat recovery steam generator



Considering the steady state analysis, ignoring heat losses from tube walls and boundaries, neglecting the radiation heat transfer rate due to the limited exhaust gas temperatures of lower than 1000 °F (538 °C) [26], and finless tubes, the thermal modeling equations for superheater, evaporator and economizer are presented in Table 1.

In this paper, a new algorithm with input parameters including the inlet hot gas mass flow rate and temperature as well as feed water temperature is presented for modeling the

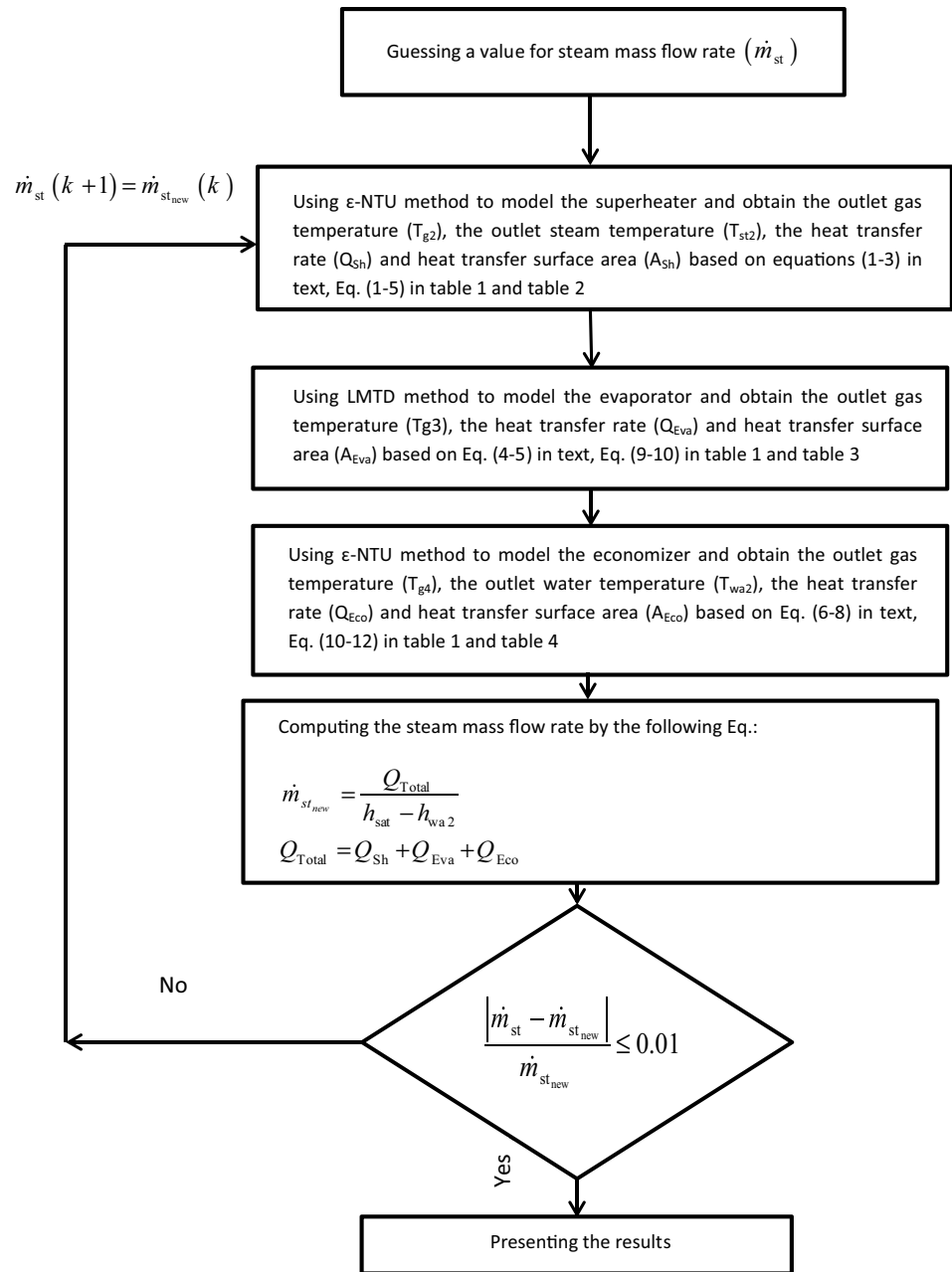
HRSG. The flowchart for computation procedure is shown in Fig. 3 and is explained in the following:

The superheater Eqs. (1 to 5 in Table 1 and 1–3 in main text) are solved assuming an initial value for the steam mass flow rate and determining the saturation temperature in drum pressure. The output parameters including the outlet gas and steam temperatures ( $T_{g2}$ ,  $T_{st}$ ) are obtained using Eqs. (2) and (3). Then, the outlet gas temperature of evaporator ( $T_{g3}$ ) is estimated using Eq. (4). Afterward, the economizer Eqs. (12 to 14

**Table 1** Relations for thermal modeling of HRSG

Equipment type	Energy balance	Description
Superheater	$\dot{m}_g C_{p_g} (T_{g1} - T_{g2}) = \dot{m}_{st} (h_{st} - h_{sat}) = \epsilon C_{Min} (T_{g1} - T_{sat})$	(1) First law of thermodynamics
	$\epsilon = 1 - \exp \left[ \frac{1 - \exp(-C^* NTU)}{-C^*} \right]$	(2) For crossflow arrangement
	$NTU = \frac{A \times U}{C_{Min}}$	(3) Non-dimensional heat transfer
	$C_{Min} = \begin{cases} C_1 = \dot{m}_g C_{p_g} & (\text{if } C_1 < C_2) \\ C_2 = \dot{m}_{st} C_{p_{st}} & (\text{if } C_2 \leq C_1) \end{cases}$	(4) Minimum heat capacity
	$\frac{1}{U} = \frac{d}{h_i d_i} + \frac{1}{h_o} + \frac{d}{2k_m} \times \ln \frac{d}{d_i} + f f_i \times \frac{d}{d_i} + f f_o$	(5) Total heat transfer coefficient
	$\epsilon = \left( \frac{T_{st} - T_{sat}}{T_{g1} - T_{sat}} \right) \times \left( \frac{C_2}{C_{Min}} \right)$	(6) This form of equations were used in optimization Part
	$NTU = \frac{-1}{C^*} \ln(1 + C^* \ln(1 - \epsilon))$	(7)
	$A = \frac{NTU \times C_{Min}}{U}$	(8)
Evaporator	$\dot{m}_g C_{p_g} (T_{g2} - T_{g3}) = FAU \Delta T_{lm}$	(9) Using LMTD method
	$\Delta T_{lm} = \frac{(T_{g2} - T_{g3})}{\ln \left( \frac{T_{g2} - T_{sat}}{T_{g3} - T_{sat}} \right)}$	(10) Logarithmic mean temperature difference with respect to the steam constant temperature during boiling process
	$T_{g3} = T_{sat} + \left[ (T_{g2} - T_{sat}) \times \exp \left( \frac{-U \times A}{\dot{m}_g C_{p_g}} \right) \right]$	(11) Inserting Eq. 10 in 9 leads to Eq. 11
Economizer	$\dot{m}_g C_{p_g} (T_{g3} - T_{g4}) = \dot{m}_{st} (h_{wa2} - h_{wa1}) = \epsilon C_{Min} (T_{g3} - T_{wa1})$	(12)
	$C_{Min} = \begin{cases} C_1 = \dot{m}_g C_{p_g} & (\text{if } C_1 < C_2) \\ C_2 = \dot{m}_{st} C_{p_{wa}} & (\text{if } C_2 \leq C_1) \end{cases}$	(13) Heat transfer in economizer using $\epsilon$ -NTU method
	$\epsilon = \left( \frac{T_{wa2} - T_{wa1}}{T_{g3} - T_{wa1}} \right) \times \left( \frac{C_2}{C_{Min}} \right)$	(14)

**Fig. 3** The flowchart for estimating the heat transfer surface area of HRSG sections (superheater, evaporator and economizer), steam generated mass flow rate and the steam outlet temperature in modeling part



in Table 1, 6–8 in main text) are solved (with the known values of  $T_{g3}$  and steam mass flow rate) and the outlet gas and outlet water temperatures from economizer ( $T_{g4}$ ,  $T_{wa2}$ ) are achieved using Eqs. (7) and (8). Therefore, the total heat transfer rate is obtained with having all gas and water temperatures and by the use of Eq. (9). Finally, the produced steam mass flow rate is obtained having the total heat transfer rate and enthalpy rise and using Eq. (10). The produced steam mass flow rate is compared with the initial assumed steam mass flow rate and the final solution is obtained by a try and error method until the convergence condition (difference value of 0.01) (Eq. 11) is reached.  $\epsilon$ -NTU method is used for superheater and economizer computations due to high convergence speed and LMTD

method is also used for evaporator since there is no need for iteration.

For superheater:

$$Q_{Sh} = \epsilon C_{\min}(T_{g1} - T_{sat}) \quad (1)$$

$$T_{g2} = T_{g1} - \left( Q_{Sh} / \dot{m}_g C_{pg} \right) \quad (2)$$

$$T_{st2} = T_{sat} + \left( Q_{Sh} / \dot{m}_{st} C_{pst} \right) \quad (3)$$

For evaporator:



$$T_{g3} = T_{sat} + (T_{g2} - T_{sat}) \exp\left(-U_{Eva}A_{Eva}/\dot{m}_g C_{pg}\right) \quad (4)$$

$$Q_{Eva} = \dot{m}_g C_{pg}(T_{g3} - T_{g2}) \quad (5)$$

For economizer:

$$Q_{Eco} = \epsilon C_{min}(T_{g3} - T_{wa1}) \quad (6)$$

$$T_{g4} = T_{g3} - (Q_{Eco}/\dot{m}_g C_{pg}) \quad (7)$$

$$T_{wa2} = T_{wa1} + (Q_{Eco}/\dot{m}_{st} C_{pwa}) \quad (8)$$

Finally:

$$Q_{Total} = Q_{Sh} + Q_{Eva} + Q_{Eco} \quad (9)$$

$$\dot{m}_{st_{new}} = Q_{Total}/(h_{sat} - h_{wa2}) \quad (10)$$

Termination condition:

$$\frac{\dot{m}_{st} - \dot{m}_{st_{new}}}{\dot{m}_{st_{new}}} \leq 0.01 \quad (11)$$

Input parameters for solving the system of Eqs. (1–8) are: the gas engine exhaust mass flow rate and temperature as well as economizer inlet water temperature. The output parameters are: inlet and outlet hot and cold fluid temperature in different HRSG sections, the produced steam mass flow rate, the total heat transfer rate and the heat transfer surface areas. With the presented algorithm, one may guess the performance parameters of water or fire tube HRSG with the least input parameters as mentioned above (without knowing pinch temperature difference, steam pressure, heat transfer surface area, etc.).

The heat transfer coefficients in superheater, evaporator and economizer are presented in Tables 2, 3 and 4, respectively.

### Exergy modeling and analysis

Exergy is the most obtainable work of a system when it reaches to the ambient condition ( $P_o, T_o$ ) from the defined state ( $P, T$ ). Irreversibility of system equipment is evaluated using exergy analysis. The equations of exergy rate and exergy destruction rate of HRSG equipment are presented in Table 5.

### Economic modeling and analysis

Total cost of HRSG is considered as investment cost due to the heat transfer surface areas.

**Table 2** The heat transfer coefficients for superheater section [26–31]

List of components	HT coefficient
Superheater (stream side)	$NU = 0.023Re^{0.8} Pr^{0.4}$
	$NU = \frac{h_i d_i}{k}$
	$Re = \left(\frac{4}{\pi}\right)\left(\frac{\dot{m}_{st}}{\mu d_i}\right)$
	$Pr = \frac{\mu C_p}{k}$
	$h_i = 0.0279 \times \frac{\dot{m}_{st}^{0.8} Y}{d_i^{1.8}}$
Superheater (gas side)	$Y = \frac{k^{0.6} C_p^{0.4}}{\mu^{0.4}}$
	$NU = 0.33Re^{0.6} Pr^{0.33}$
	$Re = \frac{Gd}{\mu}$
	$h_o = 0.33G^{0.6} \frac{Z}{d^{0.4}}$
	$Z = k^{0.67} \frac{C_p^{0.33}}{\mu^{0.27}}$
<hr/>	
	$G = \frac{\dot{m}_g}{N_w L(S_T - d)}$

$$C_{Total} = C_{CC} \quad (12)$$

Annual investment cost of HRSG directly depends on the heat transfer surface area which is computed through the following equation [34]:

$$C_{CC} = \alpha \times CRF \times (K_{Sh}A_{Sh} + K_{Eva}A_{Eva} + K_{Eco}A_{Eco}) \quad (13)$$

where CRF is capital recovery factor and is expressed by Eq. (14) and  $\alpha$  is also sum of other costs per unit of heat transfer surface area and is listed in Table 6.

$$CRF = \left(\frac{i(1+i)^n}{(1+i)^n - 1}\right) \quad (14)$$

where the parameters,  $i$  and  $n$ , are the interest rate and the equipment life time, respectively.

$K$  in Eq. (13) is the unit cost of heat transfer surface area and is available in Ref. [19].

$$\begin{aligned} K_{Sh} &= 96.2 \text{ \$/m}^2 \\ K_{Eva} &= 45.67 \text{ \$/m}^2 \\ K_{Eco} &= 34.8 \text{ \$/E}^2 \end{aligned} \quad (15)$$

The total investment cost is updated for year 2018 by the CostIndex (CI) method [34]:

$$C_{2018} = C_{old} \frac{CI_{2018}}{CI_{old}} \quad (16)$$

**Table 3** The heat transfer coefficients for evaporator section (water tube and fire tube) [26–30]

List of components	HT coefficient
Fire tube evaporator (steam side)	$h_o = 3.489q^{0.7}(0.98692P)^{0.15}$ <p>The pressure range for using the above equation is between 0 and 100 bar</p>
Fire tube evaporator (gas side)	$NU = 0.023Re^{0.8} Pr^{0.4}$ $NU = \frac{h_i d_i}{k}$ $Re = \left(\frac{4}{\pi}\right) \left(\frac{\dot{m}_g}{\mu d_i}\right)$ $Pr = \frac{\mu C_p}{k}$ $h_i = 0.0279 \times \frac{\dot{m}_g^{0.8} Y}{d_i^{1.8}}$ $G = \frac{\dot{m}_g}{N_w L(S_T - d)}$ <p>Thermo physical properties of gas must be used in the above equation</p>
Water tube evaporator (steam side)	$h_l = 0.023(k/d_i)Re^{0.8} Pr^{0.33} \left(\frac{\mu_b}{\mu_w}\right)^{0.14}$ <p>For water and <math>Re &gt; 10,000</math></p> $h_v = 0.021(k/d_i)Re^{0.8} Pr^{0.4} \left(\frac{T_b}{T_w}\right)^{0.5}$ <p>For steam and <math>Re &gt; 15,000</math></p> $h_{tp} = w_l h_l + w_v h_v$ <p>Two phase HTC</p> $\Delta T_{wall} = q \times TR$ <p>Wall temperature difference</p> $T_w = T_g - \Delta T_{Wall}$ <p>Mean wall temperature</p> $x = 1 - \frac{q}{0.00633 \times 10^6 \times h_{fg} \times d_i^{-0.1} \times (G_i/10^6)^{0.51}}$ <p>Steam quality</p> $\begin{cases} w_v = x \\ w_l = 1 - x \end{cases}$ <p>Mass coefficient of water and steam</p>

**Table 4** The heat transfer coefficients for economizer [26–30, 32, 33]

List of components	HT coefficient
Economizer (water side)	$h_i = (164.86 + 2.24 T_{wa}) \frac{V_{wa}^{0.8}}{d_i^{0.2}}$ <p><math>T_{wa}</math> is the water temperature in °C, <math>d_i</math> is the internal diameter in m and <math>V_{wa}</math> is the water velocity in m/s</p>
Economizer (gas side)	$NU = 0.33Re^{0.6} Pr^{0.33}$ $Re = \frac{Gd}{\mu}$ $h_o = 0.33G^{0.6} \frac{TF}{d^{0.4}}$ $TF = k^{0.67} \frac{C_p^{0.33}}{\mu^{0.27}}$ $G = \frac{\dot{m}_g}{N_w L(S_T - d)}$

### Optimization

Although different methods are used for optimization of energy systems such as response surface method (RSM) for optimization of pulsating heat pipe [35], fractional factorial method along with the Taguchi algorithm for optimization of a polymer exchange membrane electrolyzing

system [36], improved harmony search method (IHS) for optimization of a PV/battery hybrid unit [37], improved heuristic approach based on improved harmony search and geographic information system methods for grid-independent solar/hydrogen system optimization [38] and a hybrid heuristic technique based on simulated annealing as well as harmony search methods for optimization of solar–diesel systems [39], single-objective and multi-objective



**Table 5** Exergy relations for exergy analysis of HRSG

Equipment type	Exergy balance	Description
Superheater	$\dot{E}_{X_{in,sh}} = \dot{m}_g [(h_{g1} - h_{g2}) - T_{am}(s_{g1} - s_{g2})]$	(1) $\dot{E}_{in}$ and $\dot{E}_{out}$ are inlet and outlet exergy rate, respectively
	$\dot{E}_{X_{in,sh}} = \dot{m}_g \left[ C_{p_g} (T_{g1} - T_{g2}) - T_{am} \left( C_{p_g} \ln \left( \frac{T_{g1}}{T_{g2}} \right) - R \ln \left( \frac{P_{g1}}{P_{g1} - \Delta P_{g1}} \right) \right) \right]$	(2) With considering the combustion products as ideal gas
	$\dot{E}_{X_{out,sh}} = \dot{m}_{st} [(h_{st} - h_{sat}) - T_{am}(s_{st} - s_{sat})]$	(3) Superheater outlet exergy rate
	$\dot{E}_{Des,Sh} = \dot{E}_{X_{in,sh}} - \dot{E}_{X_{out,sh}}$	(4) Superheater exergy destruction rate
Evaporator	$\dot{E}_{X_{in,Eva}} = \dot{m}_g [(h_{g2} - h_{g3}) - T_{am}(s_{g2} - s_{g3})]$	(5)
	$\dot{E}_{X_{in,Eva}} = \dot{m}_g \left[ C_{p_g} (T_{g2} - T_{g3}) - T_{am} \left( C_{p_g} \ln \left( \frac{T_{g2}}{T_{g3}} \right) - R \ln \left( \frac{P_{g2}}{P_{g2} - \Delta P_{g2}} \right) \right) \right]$	(6)
	$\dot{E}_{X_{out,Eva}} = \dot{m}_{st} [(h_{sat} - h_{wa2}) - T_{am}(s_{sat} - s_{wa2})]$	(7)
	$\dot{E}_{Des,Eva} = \dot{E}_{X_{in,Eva}} - \dot{E}_{X_{out,Eva}}$	(8)
Economizer	$\dot{E}_{X_{in,Eco}} = \dot{m}_g [(h_{g3} - h_{g4}) - T_{am}(s_{g3} - s_{g4})]$	(9)
	$\dot{E}_{X_{in,Eco}} = \dot{m}_g \left[ C_{p_g} (T_{g3} - T_{g4}) - T_{am} \left( C_{p_g} \ln \left( \frac{T_{g3}}{T_{g4}} \right) - R \ln \left( \frac{P_{g3}}{P_{g3} - \Delta P_{g3}} \right) \right) \right]$	(10)
	$\dot{E}_{X_{out,Eco}} = \dot{m}_{wa} [(h_{wa2} - h_{wa1}) - T_{am}(s_{wa2} - s_{wa1})]$	(11)
	$\dot{E}_{Des,Eco} = \dot{E}_{X_{in,Eco}} - \dot{E}_{X_{out,Eco}}$	(12)
Gas side pressure drop	$\Delta P_g = (f_g) \frac{G^2 N_d}{500 \rho}$	(13) Gas side pressure drop
	$\rho = \frac{12.2M}{T_g}$	(14) Gas density
	$f_g = Re^{-0.15} \left[ 0.044 + \frac{0.08 (S_T/d_o)}{(S_L/d_o - 1)^{(0.43+1.13 d_0/S_L)}} \right]$	(15) Friction coefficient for inline arrangement and Reynolds between 2000 and 40,000

**Table 6**  $\alpha$  values for various costs of HRSG [12]

Items	$\alpha$ value
Heat transfer surface	1
Casing and structure	0.205
Process equipment	0.216
Piping and insulation	0.078
Control and instrumentation	0.098
Electrical panels and wiring	0.093
Engineering and inspection	0.031
Tax	0.075
Insurance	0.115
Project benefit	0.095
Other costs	0.125
Total	2.31

genetic algorithm optimization methods [2–13, 15–17, 40–42] provide appropriate results for energy system optimization. In addition, based on research finding of [43], multi-objective optimization is recommended for exergo-economic optimization of energy systems as it leads to exergy efficiency improvement and economic considerations in comparison with single-objective optimization.

Thus, in this paper, two groups of double-objective functions including total annual cost of HRSG-thermal effectiveness, and total annual cost of HRSG-exergy destruction rate are considered and used for multi-objective optimization of HRSG by the use of genetic algorithm.

**Objective functions, decision variables and constraints**

**Objective functions**

Objective functions are annual cost of HRSG (Eq. 13), exergy destruction rate of HRSG (Eq. 17):

$$\dot{E}_D = (\dot{E}_{Des,Sh} + \dot{E}_{Des,Eva} + \dot{E}_{Des,Eco}) \tag{17}$$

And thermal effectiveness of HRSG (Eq. 18):

$$\varepsilon = \frac{Q}{Q_{Max}} \tag{18}$$

$$Q = \dot{m}_g C_{p_g} (T_{g1} - T_{g4}) \tag{19}$$

$$Q_{Max} = C_{Min} (T_{g1} - T_{wa1}) \tag{20}$$

$$\begin{aligned}
 C_1 &= \dot{m}_g C_{p_g} \\
 C_2 &= \dot{m}_{st} C_{p_{wa}} \\
 C_{Min} &= \begin{cases} C_1 & (\text{if } C_1 < C_2) \\ C_2 & (\text{if } C_2 \leq C_1) \end{cases}
 \end{aligned}
 \tag{21}$$

Thermal effectiveness is the ratio of total heat transfer rate to the maximum heat transfer rate.  $C_{Min}$  is the minimum value between  $C_1$  and  $C_2$ .

**Decision variables**

Design parameters (decision variables) are pinch point temperature ( $\Delta T_{Pinch}$ ), drum pressure (for water tube boiler)/working pressure (for fire tube boiler), produced steam mass flow rate ( $\dot{m}_{st}$ ), tube length, tube diameter ( $d$ ), transverse pitch ( $S_T$ ) and longitudinal pitch ( $S_L$ ).

Output dependent parameters such as saturation steam temperature ( $T_{sat}$ ), evaporator, economizer and superheater outlet temperatures are computed with the above optimum values of design parameters. List of design parameters and their range of variation are presented in Table 7.

**Constraints**

The system constrains with respect to the operational limitations are:

1. The outlet exhaust gasses temperature must be higher than the gas dew point temperature (to prevent its water vapor condensation).
2. The gas engine power loss due to the heat recovery boiler gas side pressure drop should be lower than a determined value to prevent increase in back pressure. The power loss due to increasing the back pressure is estimated from the following relation [44]:

$$\Delta W = \dot{m}_g C_{p,g} \eta_{GE} T_3 \left[ \left( \frac{P_{atm}}{P_3} \right)^{k-1/k} - \left( \frac{P_{atm} + \Delta P}{P_3} \right)^{k-1/k} \right]
 \tag{22}$$

**Table 7** Design parameters and their range of variations [1, 12, 26]

Variable	Range of variation
$\Delta T_{Pinch}$	5–30 °C
$P_{drum}$ (water tube)	5–25 bar
Working pressure (fire tube)	5–25 bar
$\dot{m}_{st}$	1–4 kg s <sup>-1</sup>
$L$	0.5–2 m
$S_T$	63.5–152.4 mm
$S_L$	63.5–152.4 mm
$d$	38.1–76.2 mm

where  $P_3$  and  $T_3$  are pressure and temperature of the engine combustion chamber outlet gasses.

System constraints are listed in Table 8.

The procedure of optimizing fire or water tube HRSG in a gas engine cogeneration plant using two objective functions and genetic algorithm is shown in Fig. 4. It should be noted that the presented multi-objective optimization algorithm can also be utilized for HRSG in large scale combined cycle power plants by substituting a gas turbine, change of exhaust gas and mass flow rate, as well as change in the range of variation of design variables.

**Multi-objective optimization method and optimum point selection from Pareto front**

In multi-objective optimization problem, the optimum solution of one objective function differs from the optimum solution of other objective function (for example, maximizing thermal effectiveness and minimizing total annual cost in this study). Thus, the optimum answer in multi-objective method is a set of points which make a curve named Pareto front and each point on Pareto front can be final solution without dominating by other points.

Mathematical expression of multi-objective optimization problem is presented in the following:

$$\text{Find } X = X(i) \quad \forall i = 1, 2, \dots, N_{Par}
 \tag{23}$$

$$\text{Minimize Or Maximize } f_i(X) \quad \forall i = 1, 2, \dots, N_{Obj}
 \tag{24}$$

$$g_j(X) = 0 \quad \forall j = 1, 2, \dots, m
 \tag{25}$$

$$h_k(X) \leq 0 \quad \forall k = 1, 2, \dots, n
 \tag{26}$$

In our case study here, the objective functions mentioned in Eqs. (13), (17) and (18) are optimized using non-dominated sorting genetic algorithm method [45]. Thus, based on solution points on Pareto front, the designer should select the best optimum point based on the significance of each objective function using decision-making procedure. The first step in decision-making process is converting the objective functions to a non-dimensional form. Due to different dimensions

**Table 8** System constraints

Constrain	Reason
$T_{g4} > T_{dew\ point}$	Preventing condensation of water vapor in exhaust gas
$\Delta W > 0.03$	Preventing gas engine power loss due to increasing the back pressure [44]

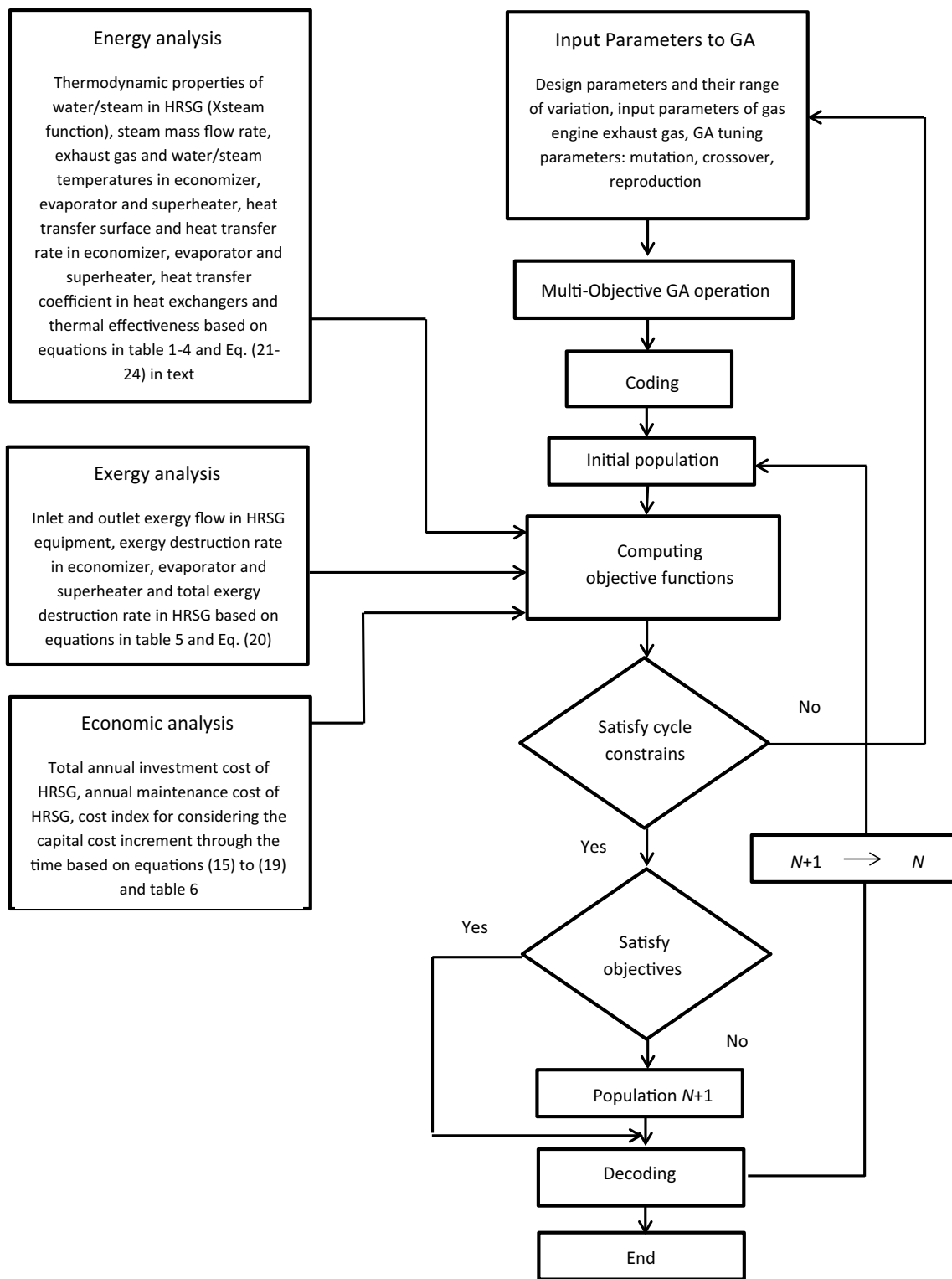


Fig. 4 The flowchart of optimizing fire/water tube HRSG in a gas engine cogeneration plant using genetic algorithm

of objective functions (total annual cost in \$/year, exergy destruction rate in kW and thermal effectiveness in %), the following equation is utilized for making objective functions non-dimensional:

$$\text{NDOB} = \frac{a_i}{\sqrt{\sum_{i=1}^n a_i^2}} \quad (27)$$

where  $a_i$  refer to the values of objective functions at each point of Pareto front.

In the second step, TOPSIS method is used for choosing the best optimum answer from Pareto front based on the closest distance from the ideal solution (in which each objective function has its best value) [46] and the farthest distance from the non-ideal solution (in which each objective function has its worst value) [47].

## Case study

1, 2 and 3 MW gas engines (with technical specification in Table 9) are used as the prime movers in gas engine cogeneration system. Advantages of applying a gas engine in CHP systems are high efficiency, relatively low investment cost, operation in partial load, fast start up, overhaul in site with ordinary operators and operation with low fuel pressure [1]. Optimum values of design variables which are mentioned in Sect. 3.1. Constant input values of parameters which are HRSG inlet gas temperature ( $T_{g1}$ ), economizer inlet water temperature ( $T_{wa1}$ ), exhaust gas dew point temperature ( $T_{\text{dew point}}$ ) and gas mass flow rate ( $\dot{m}_g$ ) are also presented in Table 9. Gas engine exhaust gas temperature and mass flow rate at partial loads are presented in Figs. 5 and 6, respectively.

## Discussion and results

### Model verification

For HRSG modeling, different section gas temperatures ( $T_{gi}$ ), economizer outlet water temperature ( $T_{wa2}$ ),

**Table 9** Constant parameters for optimization [48–50]

Parameters	1 MW	2 MW	3 MW
$T_{g1}/^{\circ}\text{C}$	462	472	540
$T_{wa1}/^{\circ}\text{C}$	64	64	64
$T_{\text{dew point}}/^{\circ}\text{C}$	105	105	105
$\dot{m}_g/\text{kg h}^{-1}$	5626	10,000	15,660

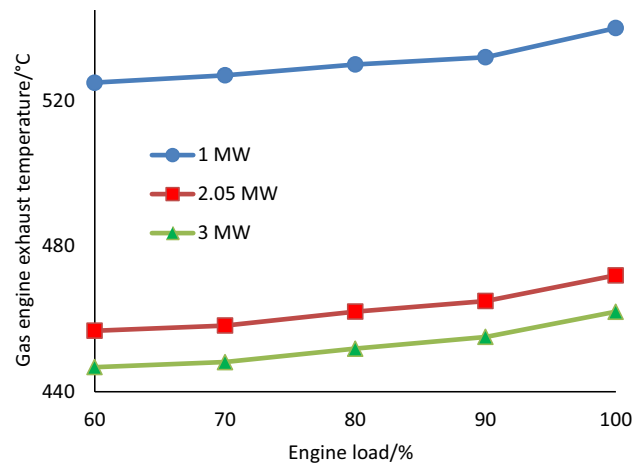


**Fig. 5** Exhaust temperature for 1, 2 and 3 MW gas engines at 60%, 70%, 80%, 90% partial and nominal (100%) loads [48–51]

superheater outlet steam temperature ( $T_{st}$ ), produced steam mass flow rate ( $\dot{m}_{st}$ ), heat transfer surface area ( $A$ ) and heat transfer rate ( $Q$ ) are obtained and compared with results generated by FireCAD™ [52]. This software can estimate economizer, evaporator and superheater thermal parameters, and thus, its results for each HRSG section are generated for verification of our modeling results. Input parameters for each section of HRSG are also presented in Table 10. The results of the present modeling and FireCAD™ are also listed in Tables 11–14. The relative error for estimating economizer and superheater parameters of fire tube and water tube evaporators are also listed in the mentioned tables. Results show that the modeling results have the maximum difference value lower than 3%, and thus, the modeling results have the accepted accuracy.

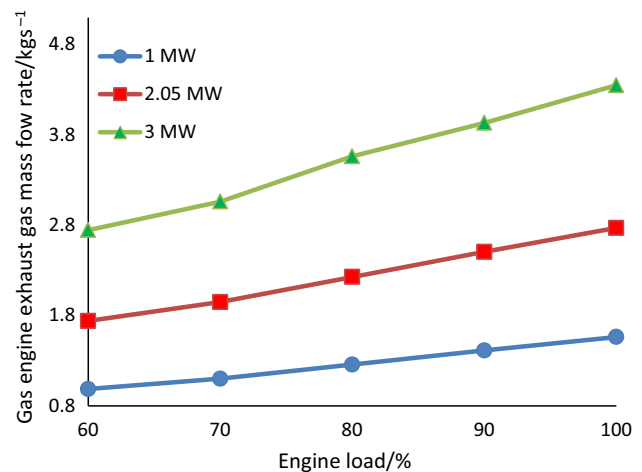


**Fig. 6** Exhaust mass flow rate for 1, 2 and 3 MW gas engines at 60%, 70%, 80%, 90% partial and nominal (100%) loads [48–51]

**Table 10** Input parameters for model verification

Inputs	$T_{g1}/^{\circ}\text{C}$	$\dot{m}_g/\text{kg h}^{-1}$	$T_{wa1}/^{\circ}\text{C}$	$P_{\text{Drum}}/\text{bar}$	Gas type
Economizer	471.66	36,287.39	20	5	Nat. gas
Superheater	471.66	36,287.39	–	5	Nat. gas
Fire tube evaporator	471.66	80,000	30	5	Nat. gas
Water tube evaporator	1038.26	35,978.41	30	5	Nat. gas

**Table 11** Verification of economizer modeling

Parameters	$T_{g4}/^{\circ}\text{C}$	$T_{wa2}/^{\circ}\text{C}$	$\dot{m}_{wa}/\text{kg h}^{-1}$	$Q_{\text{total}}/\text{kJ h}^{-1} * 10^6$	$A/\text{m}^2$
FireCad	320.71	32.00	130,926.4	6.56	98.26
Modeling	330.34	32.22	134,235.4	6.66	99.12
Relative error %	2.84	0.4	2.52	1.5	0.87

**Table 12** Verification of superheater modeling

Parameters	$T_{g2}/^{\circ}\text{C}$	$T_{st2}/^{\circ}\text{C}$	$\dot{m}_{st}/\text{kg h}^{-1}$	$Q_{\text{total}}/\text{kJ h}^{-1} * 10^6$	$A/\text{m}^2$
FireCad	182.72	354.66	29,483.5	12.39	1989.08
Modeling	180.23	357.40	29,588.8	12.20	1966.42
Relative error %	1.24	0.73	0.25	4	3

For verification of HRSG exergo-economic optimization, the results of our code for a fire tube HRSG integrated with a 600 kW micro gas turbine are obtained and compared with those reported in Ref. [12]. For this purpose, pinch temperature difference ( $\Delta T_{\text{Pinch}}$ ), length of superheater tube ( $L_{\text{Sh}}$ ), diameter of evaporator tube ( $d_{\text{Eva}}$ ), annual capital cost ( $C_{\text{Total}}$ ) and exergy destruction rate ( $\dot{E}_{\text{Destruction}}$ ) are checked for irreversibility-total annual cost objective functions with input parameters reported in Ref. [12]. The comparison of our optimization results and those reported in Ref. [12] are presented in Table 15. As the maximum difference value is about 3%, the present optimization has an acceptable accuracy.

**Optimization results**

**Pareto curves for water/fire tube HRSG**

Two pairs of double-objective functions (annual cost-thermal effectiveness and annual cost-exergy destruction rate) for water tube and fire tube boilers are selected and compared. Annual cost and exergy destruction rate are minimized, and thermal effectiveness is maximized. NSGA II optimization technique is applied by the primary generation population of 70, crossover probability of 0.7, mutation

**Table 13** Verification of fire tube evaporator modeling

Parameters	$T_{g3}/^{\circ}\text{C}$	$\dot{m}_{st}/\text{kg h}^{-1}$	$Q_{\text{total}}/\text{kJ h}^{-1} * 10^6$	$A/\text{m}^2$
FireCad	232.28	8518.51	22.53	869.35
Modeling	239.14	8473.31	22.20	845.98
Relative Error %	2.95	0.53	1.48	2.68

**Table 14** Verification of water tube evaporator modeling

Parameters	$T_{g3}/^{\circ}\text{C}$	$\dot{m}_{st}/\text{kg h}^{-1}$	$Q_{\text{total}}/\text{kJ h}^{-1} * 10^6$	$A/\text{m}^2$
FireCad	207.09	30,000	79.63	467.97
Modeling	211.33	29,918.01	77.97	458.60
Relative error %	2.04	0.27	2.08	2.01

probability of 0.4 and mutation rate of 0.02 for the solution convergence and appropriate number of iterations.

**Table 15** Comparison of results obtained from the present optimization and those reported in Ref. [12]

Parameter	Reported [12]	Present	Difference/%
$\Delta T_{\text{Pinch}}/^{\circ}\text{C}$	6.59	6.78	2.88
$L_{\text{Sh}}/\text{m}$	2.37	2.42	2.1
$d_{\text{Eva}}/\text{m}$	0.022	0.022	0
$C_{\text{Total}}/\text{\$year}^{-1}$	20.51	21.01	2.4
$\dot{E}_{\text{Des,Total}}/\text{kW}$	635.69	641.02	0.08

**Selection of optimum point on Pareto curves**

The Pareto curve with non-dimensional axes for two groups of objective functions for water tube and fire tube boilers are demonstrated in Figs. 7–10. The final optimum answer on Pareto front is chosen using TOPSIS method. As is shown in Fig. 7 (Pareto curve of annual cost-thermal effectiveness optimization for water tube boiler), the points with coordinates (38,216, 0.44) and (58,752, 0.95) have the lowest and the highest cost and thermal effectiveness, respectively. Choosing the final optimum answer from Pareto front is in relation with the significance of objective functions for the designer. For example, if designer only considers the thermal effectiveness, the best answer is (58,752, 0.95) and if he just

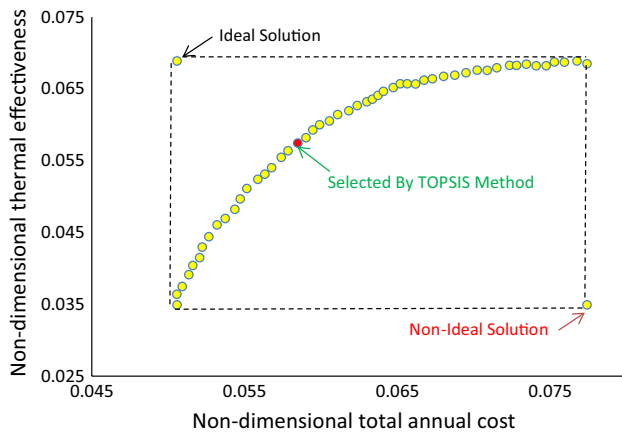


**Fig. 7** Pareto front for two objective functions (thermal effectiveness – total annual cost) optimization for water tube HRSG at nominal (100%) load of 2 MW gas engine

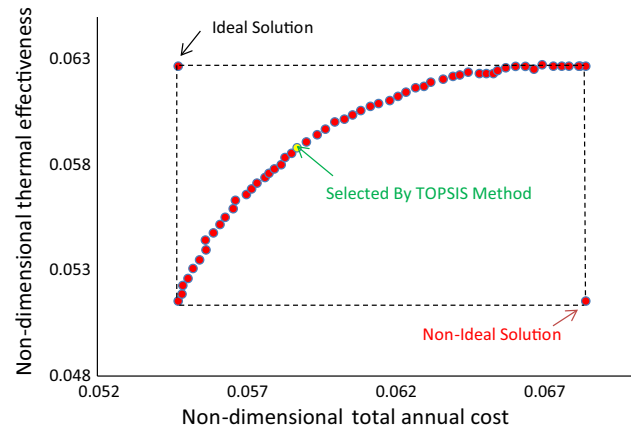


**Fig. 9** Pareto front for two objective functions (thermal effectiveness – total annual cost) optimization for fire tube HRSG at nominal (100%) load of 2 MW gas engine

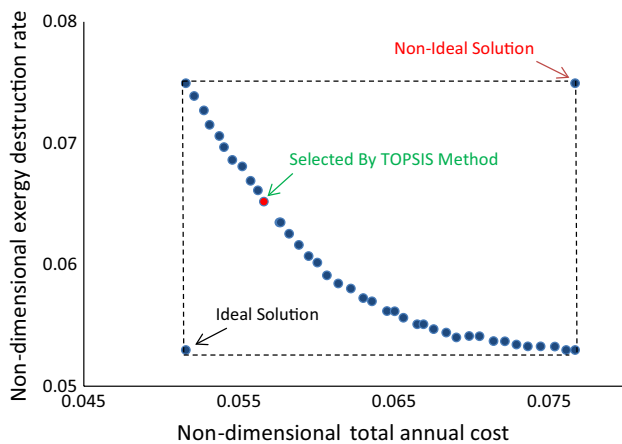


**Fig. 8** Pareto front for two objective functions (exergy destruction rate – total annual cost) optimization for water tube HRSG at nominal (100%) load of 2 MW gas engine

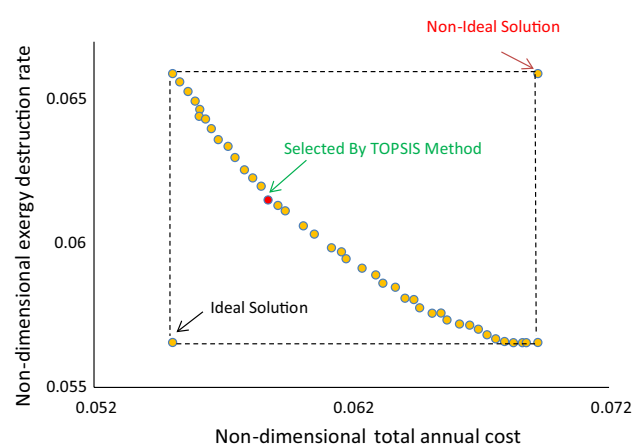


**Fig. 10** Pareto front for two objective functions (exergy destruction rate – total annual cost) optimization for fire tube HRSG at nominal (100%) load of 2 MW gas engine

considers the annual cost, the best answer is (38,216, 0.44). The Pareto curve of annual cost-exergy destruction rate for water tube boiler is shown in Fig. 8. The points with coordinates (38,200, 1795) and (58,750, 1300) have the lowest and the highest cost and exergy destruction rate, respectively.

Similar expressions are true for fire tube HRSG, the only difference refers to the lower values of objective functions for fire tube boiler (Figs. 9, 10) rather than water tube boiler.

### Optimum values of decision variables, dependent parameters and objective functions

Optimum values of design (and dependent) parameters and objective functions for two groups of objective functions (total annual cost-thermal effectiveness and total annual cost-exergy destruction rate) for 1, 2 and 3 MW gas engine

cogeneration plants at nominal (100%) load are presented in Tables 16–18. Results for 2 MW gas engine as an example are discussed and compared and similar trend occurs for 1 and 3 MW gas engines.

### Comparison of results for fire and water tube boilers

In the following sections, the optimum values of design (independent) parameters as well as dependent parameters are explained for 2 MW gas engine. The optimum values of independent and dependent parameters for one and three MW also show the same trend.

**Steam mass flow rate** As is shown in Table 16, the optimum value of the produced steam mass flow rate for water and



**Table 16** Optimum values of design variables (independent parameters) for water tube and fire tube HRSG at 1, 2 and 3 MW gas engines nominal (100%) load

Type of gas engine	Design parameters	Water tube		Fire tube	
		Cost-thermal effectiveness	Cost-exergy destruction rate	Cost-thermal effectiveness	Cost-exergy destruction rate
1 MW	$\Delta T_{\text{Pinch}}/^{\circ}\text{C}$	10.96	10.43	10.81	10.05
	$P_{\text{drum(Working)}}/\text{bar}$	9.08	9.08	9.08	9.08
	$\dot{m}_{\text{st}}/\text{kg h}^{-1}$	3539.2	3528	3540	3528
	$L/\text{m}$	0.8	0.8	0.8	0.8
	$d/\text{mm}$	50.2	50.2	50.2	50.2
	$S_{\text{T}}/\text{mm}$	69.12	69.12	69.12	69.12
	$S_{\text{L}}/\text{mm}$	93.24	91.41	88.4	86.2
2 MW	$\Delta T_{\text{Pinch}}/^{\circ}\text{C}$	12.94	11.93	12.46	11.56
	$P_{\text{drum(Working)}}/\text{bar}$	10.1	10.1	10.1	10.1
	$\dot{m}_{\text{st}}/\text{kg h}^{-1}$	6267.35	6264	6268.1	6264
	$L/\text{m}$	1	1	1	1
	$d/\text{mm}$	63.5	63.5	63.5	63.5
	$S_{\text{T}}/\text{mm}$	88.9	88.9	88.9	88.9
	$S_{\text{L}}/\text{mm}$	104.12	102.25	98.34	95.50
3 MW	$\Delta T_{\text{Pinch}}/^{\circ}\text{C}$	14.80	13.90	14.54	13.66
	$P_{\text{drum(Working)}}/\text{bar}$	12.2	12.2	12.2	12.2
	$\dot{m}_{\text{st}}/\text{kg h}^{-1}$	9944.1	9936	9945	9936
	$L/\text{m}$	1.5	1.5	1.5	1.5
	$d/\text{mm}$	75.4	75.4	75.4	75.4
	$S_{\text{T}}/\text{mm}$	99.6	99.6	99.6	99.6
	$S_{\text{L}}/\text{mm}$	110.04	108.8	105.6	104.2

fire tube boilers are close ( $6264 \text{ kg h}^{-1}$ ) for both groups of objective functions with the difference value less than 1%.

**Drum/working pressure** The optimum steam pressure and saturation temperature are close (10 bar and  $180^{\circ}\text{C}$ ) in water and fire tube boilers for both groups of objective functions with the difference value less than 0.5%.

**Pinch temperature** The optimum pinch temperature difference is close ( $12^{\circ}\text{C}$ ) in water and fire tube boilers for both pairs of objective functions with the difference value less than 1%.

**Tube length, diameter and pitch** Tube length, diameter and transversal pitch are exactly equal in water and fire tube boilers for both pairs of objective functions (1 m length, 2.5 inch diameter and 88.9 mm transverse pitch). The optimum longitudinal pitch is close in above condition with the difference value less than 3%. So it is observed that the optimum values of design parameters for both objective function pairs are close with difference value less than 3%.

**Heat transfer surface area** The values of inlet and outlet gas and steam temperatures and heat transfer surface areas for economizer, evaporator and superheater are reported in

Table 17 as independent parameters for both studied boilers. Economizer and superheater heat transfer surface areas are close for both pairs of objective functions ( $14 \text{ m}^2$  and  $30 \text{ m}^2$  for economizer and superheater, respectively, in water tube and fire tube boilers) with the difference value less than 1%. Results in Table 17 also show that the evaporator heat transfer surface area is equal for both pairs of objective functions; however, this parameter differs significantly in water tube ( $210 \text{ m}^2$ ) and fire tube ( $62 \text{ m}^2$ ) boilers. The larger heat transfer surface area in evaporator of water tube boiler causes to increase the steam production mass flow rate in this equipment.

**Gas and steam temperatures** The optimum values of inlet and outlet gas and steam temperatures for economizer, evaporator and superheater are close in water and fire tube boilers for both pairs of objective functions with the difference value less than 2%.

**The total cost** HRSG optimization considering total annual cost as the first objective function and exergy destruction rate or thermal effectiveness as the second objective function leads to the almost similar results. As is shown in Table 17, the optimum values of design and dependent parameters and

**Table 17** Dependent parameters (temperatures and heat transfer surface areas) and objective function values for water tube and fire tube HRSG for 1, 2 and 3 MW gas engines nominal (100%) load at the optimum design point

Type of gas engine	Dependent parameters	Water tube		Fire tube	
		Cost-thermal effectiveness	Cost-exergy destruction rate	Cost-thermal effectiveness	Cost-exergy destruction rate
1 MW	$A_{Sh}/m^2$	17.24	17.27	17.09	17.18
	$A_{Eva}/m^2$	119.54	119.71	35.41	35.56
	$A_{Eco}/m^2$	8.15	8.18	8.13	8.21
	$T_{g2}/^{\circ}C$	394.81	394.50	394.15	393.84
	$T_{g3}/^{\circ}C$	185.67	185.58	185.2	189.05
	$T_{g4}/^{\circ}C$	136.8	136.5	136.2	135.7
	$T_{sat}/^{\circ}C$	179.00	179.00	179.00	179.00
	$\epsilon$	0.88	0.87	0.88	0.87
	$C_{Total}/\$year^{-1}$	$225.98 * 10^2$	$226.58 * 10^2$	$113.18 * 10^2$	$114.14 * 10^2$
	$\dot{E}_{Des,Total}/kW$	766.19	769.04	761.27	765.07
2 MW	$A_{Sh}/m^2$	30.48	30.59	30.42	30.51
	$A_{Eva}/m^2$	210.27	210.02	62.65	62.40
	$A_{Eco}/m^2$	14.59	14.65	14.61	14.7
	$T_{g2}/^{\circ}C$	402.5	402.61	402.52	401.63
	$T_{g3}/^{\circ}C$	193.25	192.24	192.77	191.87
	$T_{g4}/^{\circ}C$	144.04	143.97	143.63	142.60
	$T_{sat}/^{\circ}C$	180.31	180.31	180.31	180.31
	$\epsilon$	0.91	0.90	0.91	0.90
	$C_{Total}/\$year^{-1}$	$400.54 * 10^2$	$400.56 * 10^2$	$200.20 * 10^2$	$201.04 * 10^2$
	$\dot{E}_{Des,Total}/kW$	1369.31	51,373.4	1362.1	1366.2
3 MW	$A_{Sh}/m^2$	48.45	48.5	48.32	48.39
	$A_{Eva}/m^2$	327.14	327.01	97.52	97.15
	$A_{Eco}/m^2$	22.98	23.01	22.87	22.96
	$T_{g2}/^{\circ}C$	449.61	449.19	448.95	420.63
	$T_{g3}/^{\circ}C$	237.43	237.07	236.91	202.37
	$T_{g4}/^{\circ}C$	190.96	190.61	190.24	189.9
	$T_{sat}/^{\circ}C$	188.71	188.71	188.71	188.71
	$\epsilon$	0.92	0.91	0.92	0.91
	$C_{Total}/\$year^{-1}$	$626.02 * 10^2$	$626.07 * 10^2$	$313.45 * 10^2$	$314.22 * 10^2$
	$\dot{E}_{Des,Total}/kW$	2148.01	2151.20	2138.42	2144.93

total annual cost in water tube boiler are close for both pairs of objective functions with difference value less than 3%.

With comparison of results in Table 17, it is observed that the highest cost belongs to the evaporator of water tube boiler due to the bigger heat transfer surface area of this section of HRSG. This is due to the fact that the manufacturing cost per unit of heat transfer surface area in evaporator is lower than that for superheater (Eq. 15); the optimization algorithm has selected a bigger evaporator and a smaller superheater for higher heat transfer rate and energy recovery, as well as lower total cost simultaneously. The total annual cost for two pairs of objective functions is 40,000 \$/year for water tube boiler and 20,000 \$/year for fire tube boiler.

Figures 7–10 and Table 17 show that the total annual cost of water tube HRSG is as twice as fire tube HRSG (due to the bigger evaporator heat transfer surface area) for 2 MW gas engine waste heat recovery.

**Exergy destruction rate** Table 18 shows that for 2 MW gas engine nominal power, the highest exergy destruction rate (1336.5 kW) occurs in evaporator of water tube HRSG. This is due to the significant heat transfer rate in evaporator section which results in phase change of water to steam and a significant drop of hot gas temperature due to considerable heat recovery. Economizer has the lowest value of exergy destruction rate (16.65 kW) due to the lower heat transfer rate by the hot gas to water in comparison with that for the

**Table 18** The exergy destruction rate values for water tube and fire tube HRSG for 1, 2 and 3 MW gas engines nominal (100%) load at the optimum design point

Type of gas engine	Dependent parameters	Water tube	Fire tube
1 MW	$\dot{E}_{Des,Sh}/kW$	11.6	11.56
	$\dot{E}_{Des,Eva}/kW$	748.05	743.77
	$\dot{E}_{Des,Eco}/kW$	9.48	9.74
	$\dot{E}_{Des,Total}/kW$	769.13	765.07
2 MW	$\dot{E}_{Des,Sh}/kW$	20.30	20.29
	$\dot{E}_{Des,Eva}/kW$	1336.5	1329
	$\dot{E}_{Des,Eco}/kW$	16.65	16.91
	$\dot{E}_{Des,Total}/kW$	1373.45	1366.2
3 MW	$\dot{E}_{Des,Sh}/kW$	32.01	31.95
	$\dot{E}_{Des,Eva}/kW$	2090.41	2086.34
	$\dot{E}_{Des,Eco}/kW$	25.86	26.64
	$\dot{E}_{Des,Total}/kW$	2148.28	2144.93

evaporator. The exergy destruction rate in superheater is bigger than that for economizer (20.3 kW) due to the higher heat transfer rate of hot gas and steam in superheater in comparison with that for economizer. Similar trend is observed for exergy destruction rate in fire tube boiler.

**Selection of fire tube versus water tube boiler** Comparison between water tube and fire tube HRSG shows that (with the same design and dependent parameters) the best thermodynamic efficiency (thermal effectiveness of 0.91) and the lowest exergy destruction rate (1366.2 kW which corresponds to exergy efficiency of 37.2%) are obtained with lower total annual cost (approximately 20,000 \$/year) in fire tube HRSG. This shows that with considering almost similar exergy efficiency, fire tube HRSG has 50% annual cost of water tube boiler and is a good candidate for HRSG in gas engine cogeneration plant. The lower evaporator heat transfer surface area of fire tube boiler (62 m<sup>2</sup> in comparison with that for water tube boiler, i.e., 210 m<sup>2</sup>) is due to the bigger overall heat transfer coefficient in fire tube boiler (which is about 3.4 times bigger than that for water tube boiler) and also provides the lower cost.

**Comparison of energy and exergy efficiencies as well as economic results with those in other references**

The most important performance parameters of HRSG optimization such as its energy and exergy efficiencies and pinch temperature difference are compared with those for other cogeneration plants. The optimized energy and exergy efficiencies (90% and 37.3%) of this study for water tube boiler are higher than those of [53] (72.46% and 24.89%), [54] (70.11% and 33.23%) and [55] (83% and 16%). Also the

pinch temperature difference of this study (12 °C) for fire tube boiler is slightly higher than those of [56] (5.92 °C) and [13] (9.46 °C). The higher pinch temperature difference decreases the heat transfer surface area and the total cost consequently. Thus, the presented thermo-economic multi-objective optimization provides optimum results for fire tube and water tube HRSGs with higher energy and exergy efficiencies and lower total cost.

**Performance analysis of the optimized fire tube HRSG at partial loads**

The performance of the optimized fire tube HRSG with pre-defined heat transfer surface area and geometrical parameters are thermodynamically investigated in four partial load cases (90%, 80%, 70% and 60%) for 1, 2 and 3 MW gas engines (with exhaust gas characteristics presented in Figs. 5 and 6 in case study section). The following equation is used for HRSG total heat transfer coefficient correction in gas engine partial load [57]:

$$(U)_p = (U)_d \times \left(\frac{\dot{m}_{gp}}{\dot{m}_{gd}}\right)^{0.65} \times \left(\frac{B_{gp}}{B_{gd}}\right) \times \left(\frac{\dot{m}_{stp}}{\dot{m}_{std}}\right)^{0.15} \quad (28)$$

where d is the index of design mode, p is the index of off design mode, and g and s are the indexes of gas and steam, respectively. The first, second and the third terms in the right hand of above equation are the gas mass flow rate, thermodynamic properties and steam mass flow rate corrections, respectively. Furthermore, the general equation of thermodynamic parameter variations in the form of fourth-degree polynomial is:

Ninety coefficient values of fourth-degree polynomials are obtained by curve-fitting for Figs. 11–16 to explain the behavior of different operating parameters versus engine load variations. The general form of the above mentioned fourth-degree polynomial is:

$$THP = A_4(PL)^4 + A_3(PL)^3 + A_2(PL)^2 + A_1(PL)^1 + A_0 \quad (29)$$

where THP is a thermodynamic parameter including HRSG outlet exhaust gas temperature ( $T_{g4}$ ), pinch temperature difference ( $\Delta T_{Pinch}$ ), steam generation mass flow rate ( $\dot{m}_{st}$ ), working pressure ( $P_{Working}$ ), thermal effectiveness ( $\epsilon$ ) and exergy destruction rate ( $\dot{E}_{Des,Total}$ ) and (PL) is the value of engine partial load.  $A_0$  to  $A_4$  are five constant coefficients which are obtained by curve-fitting to variations of six parameters ( $T_{g4}, \Delta T_{Pinch}, \dot{m}_{st}, P_{Working}, \epsilon, \dot{E}_{Des,Total}$ ) for 1, 2 and 3 MW gas engines (Figs. 11–16).

**HRSG exhaust gas temperature** The HRSG outlet gas temperature at 90%, 80%, 70% and 60% part loads for 1, 2 and 3 MW gas engines is shown in Fig. 11. With load reduction,

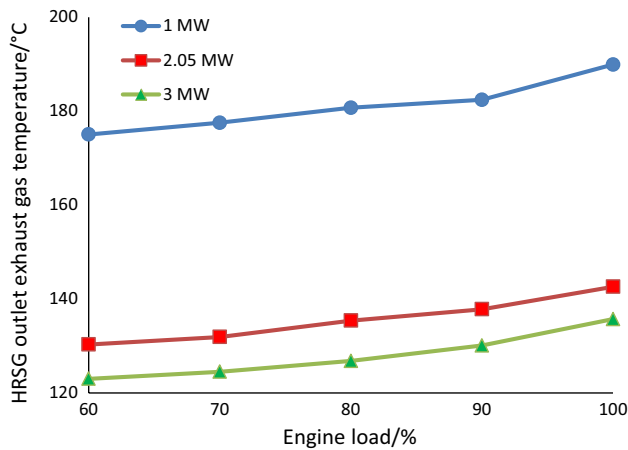


**Fig. 11** HRSG outlet exhaust gas temperature for 1, 2 and 3 MW gas engines at 60%, 70%, 80%, 90% partial and nominal (100%) loads obtained from 3E modeling and optimizing results of fire tube HRSG with fixed geometric data from Table 16

the engine exhaust gas temperature reduces which results in decrease of outlet gas temperature of HRSG.

**Pinch temperature difference** The pinch temperature difference at 90%, 80%, 70% and 60% part loads for 1, 2 and 3 MW gas engines is shown in Fig. 12. The pinch temperature difference decreases with load increment due to the increase of saturated steam pressure which causes to decrease the difference between the evaporator outlet gas temperature and the saturation steam temperature. This process makes to drop the pinch temperature difference.

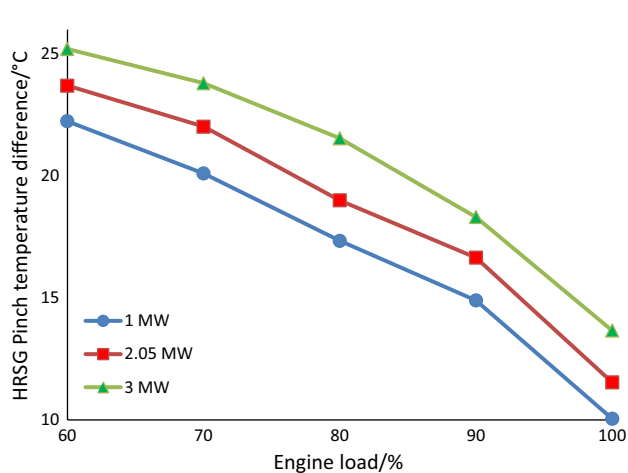


**Fig. 12** HRSG pinch temperature difference for 1, 2 and 3 MW gas engines at 60%, 70%, 80%, 90% partial and nominal (100%) loads obtained from 3E modeling and optimizing results of fire tube HRSG with fixed geometric data from Table 16

**Steam generation mass flow rate** The steam generation mass flow rate at 90%, 80%, 70% and 60% part loads for 1, 2 and 3 MW gas engines is shown in Fig. 13. The steam mass flow rate decrement by load reduction is due to decrease in the gas mass flow rate at partial load and lower heat transfer rate from hot gas to water and consequently lower vapor production.

**Working pressure** The HRSG working pressure at 90%, 80%, 70% and 60% part loads for 1, 2 and 3 MW gas engines is shown in Fig. 14. The reason of HRSG saturation (or approximately) superheat pressure decrement by load reduction is the decrease of inlet exhaust gas temperature and saturated steam generation mass flow rate at lower part loads.

**Thermal effectiveness** The HRSG thermal effectiveness at 90%, 80%, 70% and 60% part loads for 1, 2 and 3 MW gas engines is shown in Fig. 15. The reason of decrement in thermal effectiveness (Eq. 18) with load reduction decreases the inlet gas mass flow rate and consequently decreases the heat transfer rate ( $Q$ ) which leads to the decrement of the nominator in thermal effectiveness definition (Eq. 18).

**Exergy destruction rate** The exergy destruction rate at 90%, 80%, 70% and 60% part loads for 1, 2 and 3 MW gas engines is shown in Fig. 16. The decrement of exergy destruction rate at partial load operation is due to lower temperature at which heat transfer occurs as well as lower exergy flow into HRSG due to lower gas mass flow rate at part load.

Table 19 shows 90 constant coefficients (5 (coefficients)  $\times$  6 (parameters)  $\times$  3 (gas engines)) in Eq. (29) for 1, 2 and 3 MW gas engines at various part loads.

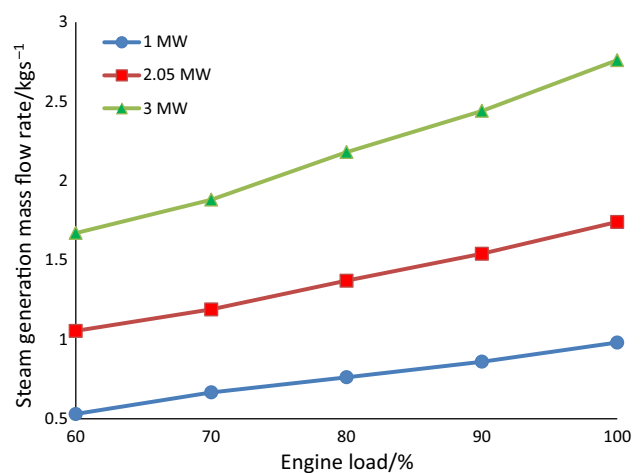


**Fig. 13** Steam generation mass flow rate for 1, 2 and 3 MW gas engines at 60%, 70%, 80%, 90% partial and nominal (100%) loads obtained from 3E modeling and optimizing results of fire tube HRSG with fixed geometric data from Table 16

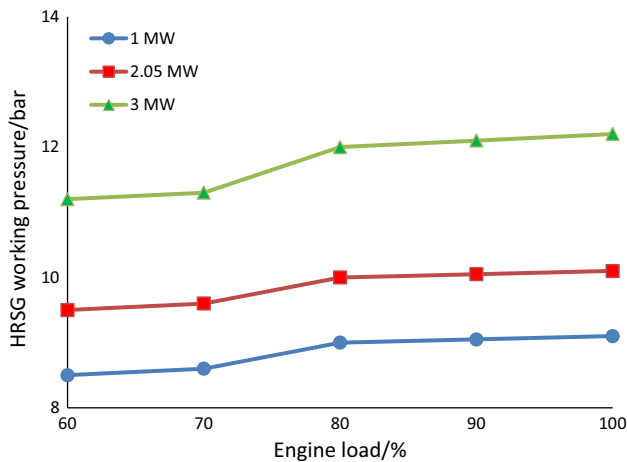


**Fig. 14** HRSG working pressure for 1, 2 and 3 MW gas engines at 60%, 70%, 80%, 90% partial and nominal (100%) loads obtained from 3E modeling and optimizing results of fire tube HRSG with fixed geometric data from Table 16

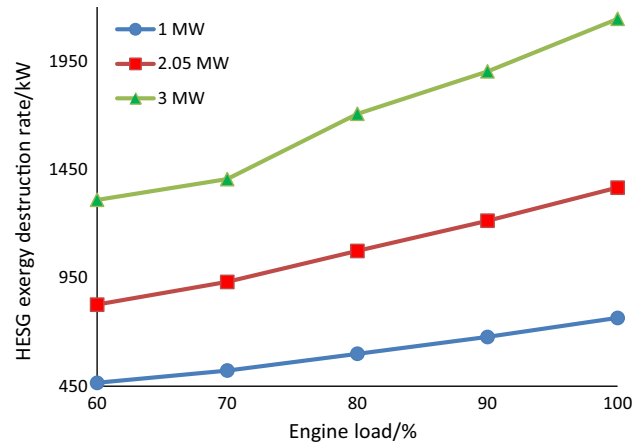


**Fig. 16** HRSG exergy destruction rate for 1, 2 and 3 MW gas engines at 60%, 70%, 80%, 90% partial and nominal (100%) loads obtained from 3E modeling and optimizing results of fire tube HRSG with fixed geometric data from Table 16

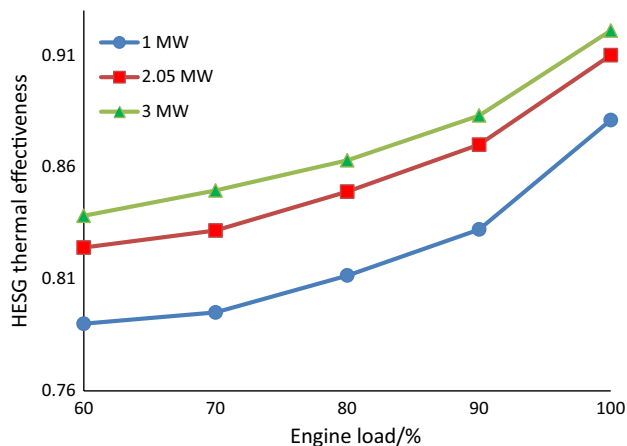


**Fig. 15** HRSG thermal effectiveness for 1, 2 and 3 MW gas engines at 60%, 70%, 80%, 90% partial and nominal (100%) loads obtained from 3E modeling and optimizing results of fire tube HRSG with fixed geometric data from Table 16

**Optimum design of HRSG for various consumption demands**

In previous sections, a robust and reliable methodology is presented in order to perform the optimum design of HRSG for heat recovery from a specific gas engine (consider as scenario A). However, due to process demands, the costumers may need an HRSG which can provide specific operational demand such as certain operating pressure or steam produced mass flow rate. In order to find the best solution for these demands, the decision variable such as operating pressure should be considered as a fixed value.

For example, if seven design parameters should be selected through the optimization process, the known value of process demand pressure can be fixed and the optimization provide other six design parameters. Results of general optimization, optimization with fixed pressure and optimization with fixed steam mass flow rate (scenarios A, B and C) for 2 MW gas engine are shown in Table 20.

**Optimum design of HRSG for a specific process pressure demand** In this scenario, operating pressure ( $P$ ) is increased to 20 bar from 10 bar obtained from thermo-economic optimization. Table 20 shows that transverse pitch ( $S_T$ ) and length of tubes ( $L$ ) and steam production rate ( $\dot{m}_{st}$ ) are almost similar to what are obtained in scenario A. However, the pinch temperature difference ( $\Delta T_{Pinch}$ ) decreases by 49.8% and reaches 5.87 °C. This decline is due to the higher saturation pressure and consequently higher saturation temperature which results in decrement of the difference between the exhaust gas and saturation steam temperature. Heat transfer surface area of evaporator ( $A_{Eva}$ ) decreases by 26.7% and reaches 42.03 m<sup>2</sup> due to higher steam pressure and temperature relative to that for scenario A (assuming equal or higher exhaust gas temperature than that in scenario A). However, the heat transfer surface area of superheater ( $A_{Sh}$ ) and economizer ( $A_{Eco}$ ) increases by 56.04% and 4.8%, respectively, to compensate the lower use of exhaust gas energy content in evaporator section and to increase the heat recovery for decreasing exergy destruction rate and increasing thermal effectiveness.

Diameter ( $d$ ) and longitudinal pitch of tubes ( $S_L$ ) decrease by 27% and 47.5% and reached 70.1 mm and 39.75 mm, respectively, which leads to a more compact configuration for heat exchangers. These lower values are selected by

**Table 19** The constant coefficients in Eq. (29) for 1, 2 and 3 MW gas engines at various partial loads

Engine type	HRSG parameters	A4	A3	A2	A1	A0
1 MW	$T_{g4}/^{\circ}\text{C}$	4E-05	-0.0123	1.4101	-71.072	1499.1
	$\Delta T_{\text{Pinch}}/^{\circ}\text{C}$	-2E-05	0.0047	-0.5483	27.708	-493
	$\dot{m}_{\text{st}}/\text{kg s}^{-1}$	-1E-07	4E-05	-0.0051	0.3101	-6.59
	$P_{\text{Working}}/\text{bar}$	8E-06	-0.0024	0.2962	-15.685	315.1
	$\epsilon$	1E-07	-4E-05	0.0047	-0.2422	5.3975
	$\dot{E}_{\text{Des, Total}}/\text{kW}$	0.0001	-0.042	5.1278	-269.83	5596.8
2 MW	$T_{g4}/^{\circ}\text{C}$	3E-05	-0.0086	1.0218	-53.062	1147.6
	$\Delta T_{\text{Pinch}}/^{\circ}\text{C}$	-2E-05	0.0071	-0.8364	42.994	-792.36
	$\dot{m}_{\text{st}}/\text{kg s}^{-1}$	4E-07	-0.0001	0.0157	-0.8188	16.54
	$P_{\text{Working}}/\text{bar}$	8E-06	-0.0024	0.2962	-15.685	316.1
	$\epsilon$	9E-08	-3E-05	0.0033	-0.1692	4.053
	$\dot{E}_{\text{Des, Total}}/\text{kW}$	0.0003	-0.0834	10.208	-538.46	11,101
3 MW	$T_{g4}/^{\circ}\text{C}$	5E-06	-0.0013	0.1505	-7.4458	258.2
	$\Delta T_{\text{Pinch}}/^{\circ}\text{C}$	-1E-06	0.0004	-0.0479	2.4888	-21.14
	$\dot{m}_{\text{st}}/\text{kg s}^{-1}$	1E-06	-0.0003	0.0371	-1.9351	38.56
	$P_{\text{Working}}/\text{bar}$	8E-06	-0.0024	0.2962	-15.675	317.2
	$\epsilon$	3E-08	-8E-06	0.0009	-0.0393	1.483
	$\dot{E}_{\text{Des, Total}}/\text{kW}$	0.0019	-0.6283	76.274	-4050.1	80,539

**Table 20** Results for optimum design of HRSG for various consumption demand including the need for specified pressure as well as steam production rate for heat recovery from a 2 W gas engine

Parameters	Scenario A: Optimum design of HRSG for 2 MW gas engine heat recovery	Scenario B: Optimum design of HRSG for demand of 20/bar pressure	Scenario C: Optimum design of HRSG for demand of 7500/kg h <sup>-1</sup> steam production rate
<i>Independent parameters</i>			
$S_T/\text{mm}$	88.9	88.9	88.9
$S_L/\text{mm}$	95.5	70.1	95.5
$L/\text{m}$	1	1	1
$\dot{m}_{\text{st}}/\text{kg h}^{-1}$	6264	6264	7500
$\Delta T_{\text{Pinch}}/^{\circ}\text{C}$	11.56	5.87	12.6
$P_{(\text{Working})}/\text{bar}$	10.1	20	11.6
$d/\text{mm}$	63.5	39.75	63.5
<i>Dependent parameters</i>			
$A_{\text{Sh}}/\text{m}^2$	30.51	47.61	33.56
$A_{\text{Eva}}/\text{m}^2$	62.4	42.03	61.89
$A_{\text{Eco}}/\text{m}^2$	14.7	15.42	16.01
$T_{g4}/^{\circ}\text{C}$	142.6	196.11	147.22
$T_{g3}/^{\circ}\text{C}$	191.87	233.78	212.86
$T_{g2}/^{\circ}\text{C}$	401.63	420	400
$T_{\text{sat}}/^{\circ}\text{C}$	180.31	227.91	200.26
<i>Objective functions</i>			
$C_{\text{Total}}/\text{\$year}^{-1}$	201.04 * 10 <sup>2</sup>	234.75 * 10 <sup>2</sup>	215.83 * 10 <sup>2</sup>
$\dot{E}_{\text{Des, Total}}/\text{kW}$	1366.2	1687.05	1445.8
$\epsilon$	0.9	0.8	0.86

genetic algorithm since it minimizes the total cost through reducing the heat transfer surface area of evaporator as the biggest heat transfer surface area of HRSG. Thus,  $A_{\text{Eva}}$

decreases by 26.7%, while  $A_{\text{Sh}}$  and  $A_{\text{Eco}}$  increase by 56.04% and 4.8%, respectively, and since the superheater has the highest price in HRSG equipment (highest manufacturing



cost per unit of heat transfer surface area, refer to Eq. 15), the total annual cost of HRSG ( $C_{\text{Total}}$ ) increases by 16% and reaches 23,475 \$/year. Exergy destruction rate ( $\dot{E}_{\text{Des, Total}}$ ) also increases by 23.48% and reaches to 1687.05 kW and thermal effectiveness ( $\epsilon$ ) decreases by 8.8% and reaches 0.8. This is due to the higher outlet exhaust gas temperature and lower evaporator heat transfer surface area which reduces the amount of recovered heat in HRSG. It can be perceived that the optimum design of HRSG for demand pressure of 20 bar has lower thermal effectiveness and higher total annual cost and exergy destruction rate than that for scenario A, but it also has higher outlet exhaust gas temperature which can be used further for heat recovery applications such as space heating or hot water consumption.

**Optimum design of HRSG for a specific steam production rate demand** In this scenario, the steam production rate ( $\dot{m}_{\text{st}}$ ) is considered a fixed value 7500 kg h<sup>-1</sup>, which is increased by 20% in comparison with that for scenario A. Table 20 shows transverse pitch ( $S_T$ ), diameter ( $d$ ) and length of tubes ( $L$ ) are similar to scenario A. Operating pressure ( $P$ ) increases by 14.8% and reaches 11.6 bar due to steam mass flow rate increment. Pinch temperature difference ( $\Delta T_{\text{Pinch}}$ ) increases by 8.9% and reaches 12.6 °C due to increase of gas temperature passing through evaporator.  $A_{\text{Eva}}$  decreases slightly (2.5%) and  $A_{\text{Sh}}$  and  $A_{\text{Eco}}$  increase by 10.12% and 8.9%, respectively, due to the similar reasons explained in scenario B. The total annual cost ( $C_{\text{Total}}$ ) also increases by 7.3% and reaches 21,583 \$/year due to the similar reasons explained in scenario B. The exergy destruction rate ( $\dot{E}_{\text{Des, Total}}$ ) also increases by 5.8% and reaches 1445.8 kW due to lower evaporator heat transfer surface area and higher saturation temperature, this is while the gas mass flow rate is equal to its value in scenario A. Thermal effectiveness ( $\epsilon$ ) decreases by 4.5% and reaches 0.86 due to the similar reasons explained in scenario B, but it has higher value than that in scenario B due to the higher steam mass flow rate.

It is observed that although the steam pressure is higher in scenario B and steam production rate is higher in scenario C, the best design occurs in scenario A in which the thermal effectiveness is higher and total annual cost and exergy destruction rate is lower. This issue confirms that the optimization procedure presented in this paper finds the best solution for the customer, but depending on the customer demand, it also can reach to an optimum design which has lower total annual cost and exergy destruction rate and higher thermal effectiveness than ordinary (non-optimized) designs.

## Conclusions

Modeling in three aspects of energy, exergy and economic and optimizing of water tube and fire tube waste heat recovery boilers (including superheater, evaporator with one pressure level and economizer) in a gas engine cogeneration plant are carried out in this paper.

In energy modeling section, the equations of  $\epsilon$ -NTU, LMTD and heat transfer coefficients for one-phase flow (for economizer and superheater) and two-phase flow (for evaporator) are organized to form a nonlinear system of equations which are used for estimating the performance parameters of a selected power output (MW) of a gas engine cogeneration plant at nominal (100%) and partial loads.

Furthermore, two pairs of double-objective functions including (total annual cost-thermal effectiveness and total annual cost-exergy destruction rate) are considered for optimization procedure with applying multi-objective non-dominated sorting genetic algorithm II (NSGA II). After optimum point selection by TOPSIS method for water tube and fire tube boilers, the results showed that using thermal effectiveness or exergy destruction rate as the second objective function beside total annual cost as the first objective function lead to the almost similar results for both HRSG. One, two and three MW gas engine cogeneration plants are studied here. The presented methodology is also utilized for optimum design of HRSG under various consumption demands including specific working pressure or steam production rate. For 2 MW gas engine as an example at nominal (100%) load, results showed that the best thermal effectiveness (0.91) and the least exergy destruction rate (approximately 1370 kW) are reached. Moreover, the total annual cost of 40,000 \$/year and 20,000 \$/year for water tube and fire tube HRSGs is obtained, respectively. Thus, choosing the fire tube HRSG decreases the costs by about 50% and consequently is more affordable for gas engine cogeneration plants. Furthermore, six relations are proposed in the form of fourth-degree polynomials for six performance parameters at nominal and partial loads. These six equations are obtained to explain the behavior of HRSG outlet exhaust gas temperature, pinch temperature difference, steam generation mass flow rate, working pressure, thermal effectiveness and exergy destruction rate versus the engine load variations. These equations can be used for specifying the operating conditions of HRSG in gas engine cogeneration plants at nominal and partial loads.

## References

- Catalog of CHP technologies. U.S. Environmental Protection Agency, Combined Heat and Power Agency partnership, Washington, D.C., United States; 2014.
- Capata R, Toro C. Feasibility analysis of a small-scale ORC energy recovery system for vehicular application. *Energy Convers Manag.* 2014;86:1078–90.
- Nadir M, Ghenaiet A. Thermodynamic optimization of several (heat recovery steam generator) HRSG configurations for a range of exhaust gas temperatures. *Energy.* 2015;86:685–95.
- Franco A, Russo A. Combined cycle plant efficiency increase based on the optimization of the heat recovery steam generator operating parameters. *Int J Therm Sci.* 2002;41:843–59.
- Rezaei A, Tsatsaronis G, Hellwig U. Thermal design and optimization of a heat recovery steam generator in a combined-cycle power plant by applying a genetic algorithm. *Energy.* 2019. <https://doi.org/10.1016/j.energy.2018.11.047>.
- Carapellucci R, Giordano L. A comparison between exergetic and economic criteria for optimizing the heat recovery steam generators of gas-steam power plants. *Energy.* 2013;58:458–72.
- Nadir M, Ghenaiet A, Carasci C. Thermo-economic optimization of heat recovery steam generator for a range of gas turbine exhaust temperatures. *Appl Therm Eng.* 2016;106:811–26.
- Kaviri AG, Jaafar MN, Lazim TM, Barzegaravval H. Exergoenvironmental optimization of heat recovery steam generators in combined cycle power plant through energy and exergy analysis. *Energy Convers Manag.* 2013;67:27–33.
- Nikbakht Naserabad S, Mehrpanahi A, Ahmadi G. Multi-Objective optimization of HRSG configurations on the steam power plant repowering specifications. *Energy.* 2018. <https://doi.org/10.1016/j.energy.2018.06.130>.
- Ahmed A, Esmaeil KK, Irfan MA, Al-Mufadi FA. Design methodology of heat recovery steam generator in electric utility for waste heat recovery. *Int J Low-Carbon Technol.* 2018. <https://doi.org/10.1093/ijlct/cty045>.
- Mokhtari H, Ahmadiesedigh H, Ameri M. The optimal design and 4E analysis of double pressure HRSG utilizing steam injection for Damavand power plant. *Energy.* 2017;118:399–413.
- Behbahani-nia A, Bagheri M. Optimization of fire tube heat recovery steam generators for cogeneration plants through genetic algorithm. *Appl Therm Eng.* 2010;30:2378–85.
- Najafi H, Najafi B. Multi-objective optimization of a fire-tube heat recovery steam generator system. In: *IEEE Electrical Power & Energy Conference*; 2009.
- Masum BM, Masjuki HH, Kalam MA, Palash SM, Habibullah M. Effect of alcohol–gasoline blends optimization on fuel properties, performance and emissions of a SI engine. *J Clean Prod.* 2014. <https://doi.org/10.1016/j.jclepro.2014.08.032>.
- Terhan M, Comakli K. Energy and exergy analyses of natural gas-fired boilers in a district heating system. *Appl Therm Eng.* 2017;121:380–7.
- Sharma M, Singh O. Exergy analysis of the dual pressure HRSG for varying physical parameters. *Appl Therm Eng.* 2017;114:993–1001.
- Ahmadi Gh, Toghraie D, Ali Akbari O. Technical and environmental analysis of repowering the existing CHP system in a petrochemical plant: a case study. *Energy.* 2018. <https://doi.org/10.1016/j.energy.2018.06.208>.
- Maleki A, Thi Ngo PT, Irandoost Shahrestani M. Energy and exergy analysis of a PV module cooled by an active cooling approach. *J Therm Anal Calorim.* 2020. <https://doi.org/10.1007/s10973-020-09916-0>.
- Casarosa C, Donatini F. Thermoeconomic optimization of heat recovery steam generators operating parameters for combined plants. *Energy.* 2004;29:389–414.
- Chen B, Guo Q, Chen Y, Sun H. An economic dispatch model for combined heat and power systems considering the characteristics of heat recovery steam generators. *Electric Power Energy Syst.* 2020;118:1–9.
- Carcascia C, Pacificia B, Winchlera L, Cosib L, Ferrarob R. Thermoeconomic analysis of a one-pressure level heat recovery steam generator considering real steam turbine cost. *Energy Procedia.* 2015;82:591–8.
- Li J, Mohammadi A, Maleki A. Techno-economic analysis of new integrated system of humid air turbine, organic Rankine cycle, and parabolic trough collector. *J Therm Anal Calorim.* 2019. <https://doi.org/10.1007/s10973-019-08855-9>.
- Hossain ShN, Bari S. Waste heat recovery from the exhaust of a diesel generator using Rankine Cycle. *Energy Convers Manag.* 2013;75:141–51.
- Hossain ShN, Bari S. Waste heat recovery from the exhaust of a diesel generator using shell and tube heat exchanger. In: *ASME International Mechanical Engineering Congress and Exposition*, San Diego, California, USA, 15–21 November 2013.
- Pandiyarajan V, Ch Pandian M, Malan E, Velraj R, Seeniraj RV. Experimental investigation on heat recovery from diesel engine exhaust using finned shell and tube heat exchanger and thermal storage system. *Appl Energy.* 2011;88:77–87.
- Ganapathy V. *Industrial boilers and heat recovery steam generators: design, applications and calculations.* 3rd ed. New York: Marcel Dekker Inc; 2003.
- Bejan A, Tsatsaronis G, Moran M. *Thermal design and optimization.* New York: Wiley; 1996.
- Oliveira RD, Rodriguez CA, Coronado CJ, Nascimento MA. Technical and economic analyses of waste heat energy recovery from internal combustion engines by the organic Rankine cycle. *Energy Convers Manag.* 2016;129:168–79.
- Roshenow W, Hartnett JP. *Handbook of heat transfer.* New York: McGraw-Hill; 1972. p. 13–56.
- Kakac S, Liu H, Pramuanjaroenkij A. *Heat exchangers selection, rating and thermal design.* 3rd ed. Boca Raton: CRC Press; 2012.
- Cao Y, Nguyen PT, Jermstittiparsert K, Belmabrouk H, Alharbi SO, Khorasani MS. Thermal characteristics of air–water two-phase flow in a vertical annularly corrugated tube. *J Energy Storage.* 2020. <https://doi.org/10.1016/j.est.2020.101605>.
- Tian XX, Asaadi S, Moria H, Kaood A, Pourhedayat S, Jermstittiparsert K. Proposing tube-bundle arrangement of tubular thermoelectric module as a novel air cooler. *Energy.* 2020. <https://doi.org/10.1016/j.energy.2020.118428>.
- Bahmani MH, Akbari OA, Alrashed AA, Sheikhzadeh G, Zarringhalam M, Ahmadi-Sheikh-Shabani G, Goodarzi M. Investigation of turbulent heat transfer and nanofluid flow in a double pipe heat exchanger. *Adv Powder Technol.* 2017. <https://doi.org/10.1016/j.apt.2017.11.013>.
- Turton R, Bailie RC, Whiting WB, Shaeiwitz JA. *Analysis, synthesis, and design of chemical processes.* 3rd ed. Upper Saddle River: Prentice Hall; 2009.
- Li Z, Sarafraz MM, Mazinani A, Moria H, Tlili I, Alkanhal TA, Goodarzi M, Safaei MR. Operation analysis, response and performance evaluation of a pulsating heat pipe for low temperature heat recovery. *Energy Convers Manag.* 2020. <https://doi.org/10.1016/j.enconman.2020.113230>.
- Toghyani S, Fakhradini S, Afshar E, Baniasadi E, Abdollahzadeh Jamalabadi MY, Safdari Shadloo M. Optimization of operating parameters of a polymer exchange membrane electrolyzer. *Int J Hydrogen Energy.* 2019. <https://doi.org/10.1016/j.ijhydene.2019.01.186>.

37. Maleki A, Nazari MA, Pourfayaz F. Harmony search optimization for optimum sizing of hybrid solar schemes based on battery storage unit. *Energy Rep.* 2020. <https://doi.org/10.1016/j.egy.2020.03.014>.
38. Zhang G, Shi Y, Maleki A, Rosen MA. Optimal location and size of a grid-independent solar/hydrogen system for rural areas using an efficient heuristic approach. *Renew Energy.* 2020. <https://doi.org/10.1016/j.renene.2020.04.010>.
39. Cai W, Li X, Maleki A, Pourfayaz F, Rosen MA, Nazari MA, Bui DT. Optimal sizing and location based on economic parameters for an off-grid application of a hybrid system with photovoltaic, battery and diesel technology. *Energy.* 2020. <https://doi.org/10.1016/j.energy.2020.117480>.
40. Pourfayaz F, Shirmohammadi R, Maleki A, Kasaeian A. Improvement of solar flat-plate collector performance by optimum tilt angle and minimizing top heat loss coefficient using particle swarm optimization. *Energy Sci Eng.* 2020. <https://doi.org/10.1002/ese3.693>.
41. Sadeghi S, Maghsoudi P, Shabani B, Haghshenas Gorgani H, Shabani N. Performance analysis and multi-objective optimization of an organic Rankine cycle with binary zeotropic working fluid employing modified artificial bee colony algorithm. *J Therm Anal Calorim.* 2018. <https://doi.org/10.1007/s10973-018-7801-y>.
42. Ahmadi B, Golneshan AA, Arasteh H, Karimipour A, Vu Bach Q. Energy and exergy analysis and optimization of a gas turbine cycle coupled by a bottoming organic Rankine cycle. *J Therm Anal Calorim.* 2019. <https://doi.org/10.1007/s10973-019-09088-6>.
43. Tian MW, Parikhani T, Jermisittiparsert K, Ashraf MA. Exergo-economic optimization of a new double-flash geothermal-based combined cooling and power (CCP) system at two different cooling temperatures assisted by boosters. *J Clean Prod.* 2020. <https://doi.org/10.1016/j.jclepro.2020.120921>.
44. Franco A, Giannini N. A general method for the optimum design of heat recovery steam generators. *Energy.* 2006;31:3342–61.
45. Srinivas N, Deb K. Multiobjective optimization using nondominated sorting in genetic algorithms. *Evol Comput.* 1994;2:221–48.
46. Srinivasan V, Shocker AD. Linear programming techniques for multidimensional analysis of preference. *Psychometrika.* 1973;38:337–42.
47. Yue Zh. A method for group decision-making based on determining weights of decision makers using TOPSIS. *Appl Math Model.* 2011;35:1926–36.
48. [https://www.cat.com/en\\_US/products/new/power-systems/industrial/gas-engines.html](https://www.cat.com/en_US/products/new/power-systems/industrial/gas-engines.html).
49. Wang X, Shu G, Tian H, Feng W, Liu P, Li X. Effect factors of part-load performance for various organic Rankine cycles using in engine waste heat recovery. *Energy Convers Manag.* 2018;174:504–15.
50. <https://www.mwm.net/mwm-kwk-bhkw/gasmotorenstromaggregate/gasmotor-tcg-2032/>.
51. Lecompte S, Huisseune H, van den Broek M, Schampheleire S, Paeppe M. Part load based thermo-economic optimization of the Organic Rankine Cycle (ORC) applied to a Combined Heat and Power (CHP) system. *Appl Energy.* 2013;111:871–81.
52. <https://firecad.net/fire-tube-boiler-design-software/>.
53. Saidur R, Ahamed JU, Masjuki HH. Energy, exergy and economic analysis of industrial boilers. *Energy Policy.* 2010;38:2188–97.
54. Oladiran MT, Meyer JP. Energy and exergy analyses of energy consumptions in the industrial sector in South Africa. *Appl Energy.* 2007;84:1056–67.
55. Utlu Z, Hepbasli A (2007) A review and assessment of the energy utilization efficiency in the Turkish industrial sector using energy and exergy analysis method. *Renew Sustain Energy Rev.* 2007;11:1438–59.
56. Bahrampoury R, Behbahaninia A. Multi-objective optimization of heat recovery steam generators. *Energy Equip Syst.* 2014;2:129–40.
57. Ganapathy V. *Steam generators and waste heat boilers for process and plant engineers.* Boca Raton: CRC Press; 2014.

**Publisher's Note** Springer Nature remains neutral with regard to jurisdictional claims in published maps and institutional affiliations.